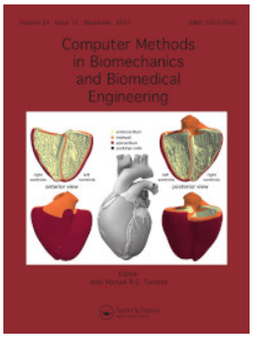

Taylor & Francis
Taylor & Francis Group

Computer Methods in Biomechanics and Biomedical Engineering

ISSN: (Print) (Online) Journal homepage: https://www.tandfonline.com/loi/gcmb20

Patient-specific fluid–structure interaction model of bile flow: comparison between 1-way and 2-way algorithms

Alex G. Kuchumov, Vasily Vedeneev, Vladimir Samartsev, Aleksandr Khairulin & Oleg Ivanov

To cite this article: Alex G. Kuchumov, Vasily Vedeneev, Vladimir Samartsev, Aleksandr Khairulin & Oleg Ivanov (2021) Patient-specific fluid–structure interaction model of bile flow: comparison between 1-way and 2-way algorithms, Computer Methods in Biomechanics and Biomedical Engineering, 24:15, 1693-1717, DOI: 10.1080/10255842.2021.1910942

To link to this article: https://doi.org/10.1080/10255842.2021.1910942

COMPUTER METHODS IN BIOMECHANICS AND BIOMEDICAL ENGINEERING
2021, VOL. 24, NO. 15, 1693–1717
https://doi.org/10.1080/10255842.2021.1910942

Patient-specific fluid–structure interaction model of bile flow: comparison between 1-way and 2-way algorithms

Alex G. Kuchumov[a,b], Vasily Vedeneev[c,d], Vladimir Samartsev[e], Aleksandr Khairulin[a] and Oleg Ivanov[f]

[a]Department of Computational Mathematics, Mechanics, and Biomechanics, Perm National Research Polytechnic University, Perm, Russian Federation; [b]Mathematical Center, Kazan Federal University, Kazan, Russian Federation; [c]Steklov Mathematical Institute of Russian Academy of Sciences, Moscow, Russian Federation; [d]Institute of Mechanics, Moscow, Russian Federation; [e]Department of General Surgery, Perm State Medical University, Perm, Russian Federation; [f]Institute of Mechanics of Moscow State University, Moscow, Russian Federation

ABSTRACT

Gallbladder disease is one of the most spread pathologies in the world. Despite the number of operations dealing with biliary surgery increases, the number of postoperative complications is also high. The aim of this study is to show the influence of the biliary system pathology on bile flow character and to numerically assess the effect of surgical operation (cholecystectomy) on the fluid dynamics in the extrahepatic biliary tree, and also to reveal the difference between 1-way and 2-way FSI algorithms on the results. Moreover, the bile viscosity and biliary tree geometry influence on the choledynamics were evaluated. Bile velocity, pressure, wall shear stress (WSS), displacements and von Mises stress distributions in the extrahepatic biliary tree are presented, and comparison is made between a healthy and a lithogenic bile. The patient-specific biliary tree model is created using magnetic resonance imaging (MRI) and imported in a commercial finite element analysis software. It is found that in the case of lithogenic bile, velocities have lower magnitude while pressures are higher. Furthermore, stress analysis of the bile ducts shows that the WSS distribution is found mostly prevailing in the common hepatic duct and common bile duct areas. It is shown that when it is necessary to evaluate the bile flow dynamics in urgent medical situations, 1-way analysis is acceptable. Nevertheless, 2-way FSI provides more accurate data, if necessary to evaluate the stress–strain state of bile ducts. The proposed model can be applied to medical practice to reduce the number of post-operative complications.

ARTICLE HISTORY
Received 8 March 2019
Accepted 28 March 2021

KEYWORDS
Extrahepatic biliary tree; choledynamics; patient-specific modelling

1. Introduction

The process of gallstone formation is referred to gallbladder disease (Diehl 1991; Stinton and Shaffer 2012). Gallstones develop when substances in the bile (such as cholesterol, bilirubin and bile salts) form hard particles that block the passageway to the gallbladder (Diehl 1991). It means that bile changes its structural and rheological properties, which in this case is called 'lithogenic bile' (i.e. a bile that tends to generate gallstones). Also, gallstones, which can be as large as a golf ball (Mohan et al. 2014), tend to form when the gallbladder does not empty completely.

Gallstones affect 10% to 15% of the adult population in the United States (Stinton and Shaffer 2012) and the United Kingdom (Luo et al. 2007), respectively, and 12–20% in Russia (Marakhovskiy 2003). The presence of gallstones may lead to different complications starting from bile duct inflammation to lethal cases such as gallbladder cancer (Opie 1901; Portincasa et al. 2006). Biomechanical and choledynamic factors (including bile flow dynamics, gallbladder and ducts contraction, pressure gradients' shift due to pathology) have crucial influence on gallstones formation (Luo et al. 2007). It is known that prolonged bile stasis in the gallbladder due to the biomechanical factors mentioned above can lead to gallstone formation along with the metabolic liver disorders.

The two major types of gallstones are (1) cholesterol stones, associated with cholesterol supersaturation in the bile, and (2) pigment stones (subdivided into brown and black types), associated with result from conditions in which unconjugated bilirubin levels are elevated.

CONTACT Alex G. Kuchumov kychymov@inbox.ru
Supplemental data for this article is available online at https://doi.org/10.1080/10255842.2021.1910942.

Other risk factors for gallstone formation are female gender (gallstones are twice as common in women compared with men), obesity, estrogen supplementation, multiparous state, advancing age, hyperlipidemia, inborn disorders of bile metabolism, and family history of gallstones (Kay Washington 2009).Cholecystectomy is the most commonly performed abdominal operation for the treatment of patients suffering from gallbladder disease in Western countries (Ooi et al. 2004). Nevertheless, the operation outcome is not always positive (Kuchumov et al. 2011; Mohan et al. 2014) including bile duct injury; injuries to the intestine, bowel and blood vessels; bile leakage; deep vein thrombosis (Khan et al. 2007). Serious complications result in part from patient state, surgical inexperience, and the technical constraints.

Moreover, a surgeon can not predict a change of body functional recovery (the daily bile flow rate, pressure in the biliary system segments, wall shear stress, etc.) in the post-operational period. In order to understand the causes of diseases, it is important to carry out the physiological and mechanical description of the human biliary system behaviour.

Computational simulations, which would account for the dynamic interaction between the choledynamics and wall deformation, are known as fluid–structure interaction (FSI) simulations, providing realistic results to obtain relevant choledynamic factors. Numerical and analytical CFD models applied to bile flow study have been proposed by several research groups (Ooi et al. 2004; Li et al. 2007; Li et al. 2008a; Maiti and Misra 2011; Agarwal et al. 2012a; Kuchumov et al. 2013a, 2014; Lo et al. 2015; Agarwal and Singh 2016).

Ooi et al. (2004) proposed two-dimensional and three-dimensional computational models of the bile flow in the cystic duct considered as a channel with baffles. It was found that the most significant geometric factors that regulate the hydraulic resistance of the cystic duct are the height and number of baffles.

Agarwal et al. (2012a) developed a mathematical model of the flow of bile as a Herschel – Bulkley fluid in the stenosed channel. Changes in a flow resistance with stone dimensions and shear stresses were presented.

Further, Li et al. (2007) proposed an analytical model of the flow of bile in the biliary tree as a T-shaped tube with rigid and flexible walls. After that, these authors proposed a model of the bile flow as a Newtonian and non-Newtonian fluid in the three-dimensional geometry of the cystic duct, taking into account the fluid–structure interaction (Li et al. 2008a).

Maiti and Misra (2011) presented a model of peristaltic transport in the common bile duct with stones as a porous channel for studying the influence of various factors on reflux. In the presence of gallstones, it has been found that the rate of bile increases with an increase in the porosity parameter, while the critical pressure for reflux decreases with increasing porosity.

Lo et al. (2015) presented a model including cystic duct model, Poiseuille–Hagen law law and round jet along with optical flow system to study bile reflux. Using this method, physicians may estimate the quantity of bile reflux and observe bile flow to determine whether or not it moves into the stomach.

Kuchumov et al. (2013a) proposed a model of bile flow in the channel with a stone. As a result of solving the problem, the bile velocity profile, flow rate vs. time, and bile pressure vs. calculus radius were obtained. The dependences obtained may play an important role in the assessment of an indication to operation.

It should be noted that in the majority of works, the models of bile flow in separate segments were considered only and the entire model of the flow in the biliary system was not taken into account. Also, they did not take into account a patient-specific geometry of bile ducts and their compliance, influence of the gallbladder and peristalsis of the major duodenal papilla.

Also, researchers have investigated bile flow in different ducts by taking into account the peristaltic wave propagation, which plays an important role in fluid transport (Kuchumov et al. 2015; Kuchumov 2016).

A thorough review of current publications in this field reveals that bile flow has been mostly investigated in separate ducts of the biliary system. Some attempts to make patient-specific models of cystic ducts (e.g. Al-Atabi et al. 2012) and the entire biliary system (e.g. (Kuchumov et al. 2013b; Kuchumov 2019) and (Bhuvana and Anburajan 2013) have been made. So far, however, there has been no attempt to create a patient-specific model of bile flow and perform FSI simulations.

Recently, fluid-structure interaction analysis has utilized as a tool that combines CFD analysis with stress-strain state evaluation to evaluate the influence of fluid flow to the surrounding vessels and tissues, and vice versa. FSI has a rapidly growing potential compared to CFD analysis in biomedical engineering. A numerous studies were performed to reveal the mechanical behaviour of blood vessels (Jahanzamin et al. 2019; Oliveira et al. 2019; Qiao et al. 2019; Xu et

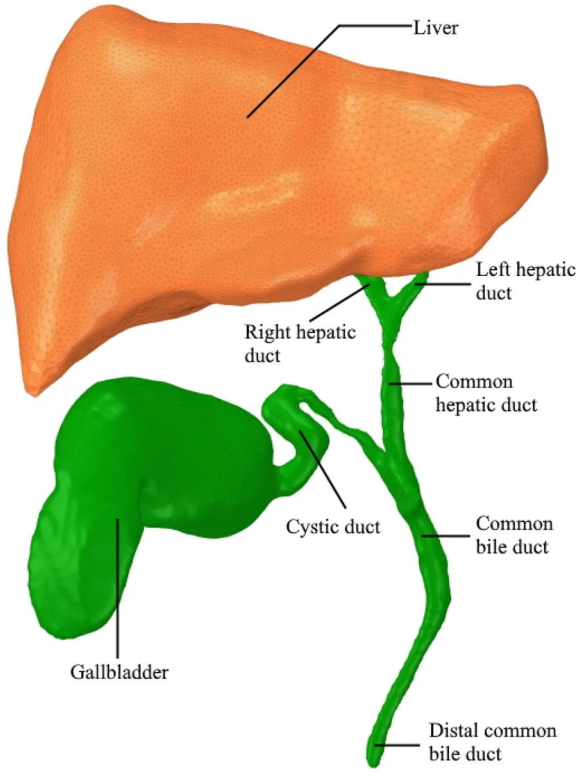

(I)

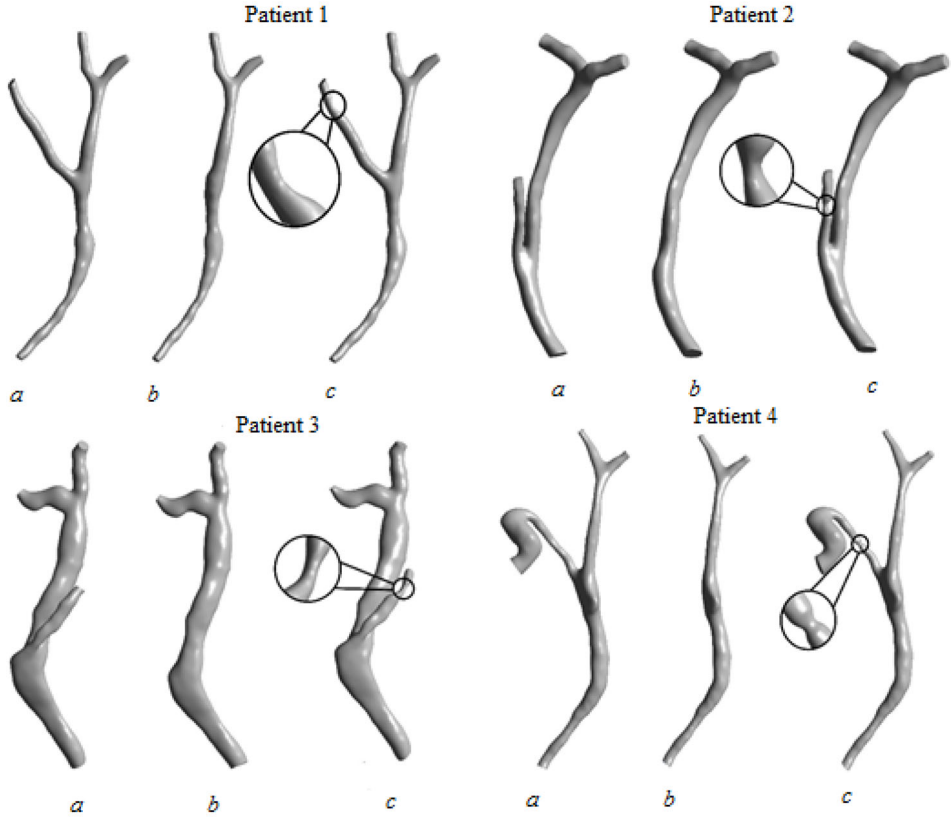

(II)

Figure 1. Biliary system scheme (I) and geometries of 4 patients: (a) healthy state biliary system, (b) model without cystic ducts (cholecystectomy case), (c) stone presence in the cystic duct (II).

al. 2020). These studies demonstrate the necessity for advanced numerical and mathematical patient-specific models at the healthy state and pathology. FSI assumes two approaches: one-way FSI and two-way FSI.

A one-way FSI (also called one-direction FSI) assumes that results from the fluid model are transferred to the solid model only once as an external load (Ahamed et al. 2017). But in the case of two-way FSI, the load mapping is performed in an iterative loop, that is, the results (e.g. pressure) of the fluid model are transferred to the solid model and the results (e.g. deformations) of the solid model are, in turn, transferred back to the fluid model to influence the behaviour of the fluid part. This iterative process will continue until convergence is found or the process is manually stopped (Ezkurra et al. 2018).

Comparison between 1-way and 2-way FSI approaches is still a challenging task. On the one hand, 1-way FSI utilization can be a good compromise that provides more realistic loading conditions for patient-specific biofluid analysis and clinical applications, where time analysis plays a crucial role (Tao et al. 2015). On the other hand, two-way FSI is more accurate and can bring results that are more accurate. A proper choose of the approach for the current biomedical problem can significantly reduce the computational costs and provide accurate results with minimal implementation effort.

The aim of the present paper is to develop a computational approach to model a patient-specific bile flow using an FSI model for the following four cases:

- a: healthy bile flow considered as Newtonian fluid;
- b: lithogenic bile considered as non-Newtonian Carreau fluid;
- c: lithogenic bile flow in the biliary tree after cholecystectomy;
- d: lithogenic bile flow in the biliary tree in case of a stone in the cystic duct.

Also, we perform the comparison between 1-way and 2-way FSI algorithms to show, which approach is more effective for the clinical practice from reliability and usefulness point of view.

2. Materials and methods

2.1. Patient models

Geometric models of 4 patients were obtained by processing CT scans (Figure 1). The images were imported into ITK-SNAP software (ITK-Snap, USA).

Table 1. The meshes used for the mesh independency tests.

Domains	Mesh 1	Mesh 2	Mesh 3	Mesh 4
Fluid	511,765	872,383	1,297,023	1,568,128
Solid	60,274	79,018	209,946	315,645

After that, the biliary system segmentation was performed. Then, each geometry model was processed in the ANSYS SPACECLAIM package (ANSYS, Inc., Canonsburg, Pennsylvania, USA). These geometries are referred to as 'healthy'; the same geometry was also used for modelling of lithogenic bile flow. Additional modeling was performed to obtain cholecystectomy models and models with stone presence (local narrowing of biliary ducts).

2.2. Meshing

Fluid and solid domains were meshed using ANSYS ICEM 19.0 (ANSYS, Inc., Canonsburg, Pennsylvania, USA).

The convergence of the numerical solution is analysed for the case of normal bile flow. The chosen convergence parameters were momentum and mass. Several variants of the finite element mesh were considered during the convergence analysis. The information related to the mesh is presented in Table 1. The minimum size of the element either for solid or for fluid mesh was calculated from the smallest overall size of the structure. The mesh refinement was made on the bifurcation site and different ducts of the biliary tree. The convergence analysis enabled choosing the optimal mesh element size. While all the meshes led to the converged solution since the difference in results of the computations (where the maximum velocity was chosen as a monitor in case of fluid flow, pressure, and wall shear stress and wall displacement and von Mises stress for the solid domain, respectively) were negligible in the case of mesh 3 and mesh 4 (less than 2%). A mesh convergence study was performed to ensure that the uncertainty associated with spatial discretization is not significant. It took more time to simulate the latter mesh, but the differences in the results were negligible, thus it can be concluded that results are independent of the mesh. Comparison between solid and fluid meshes is presented in Figure 2(c). Figure 2(d–f) consists the data for velocity, pressure, wall shear stress values depending on the mesh elements.Finally, mesh 3 was chosen for subsequent analysis. Thus, fluid and solid meshes consisted of 1,297,023 and 209,946 elements, respectively, and were used for the final computations (Figure 2(a,b)).

The optimal fluid mesh was a five-layer mesh with the thickness of the first layer 0.2 mm, the growth

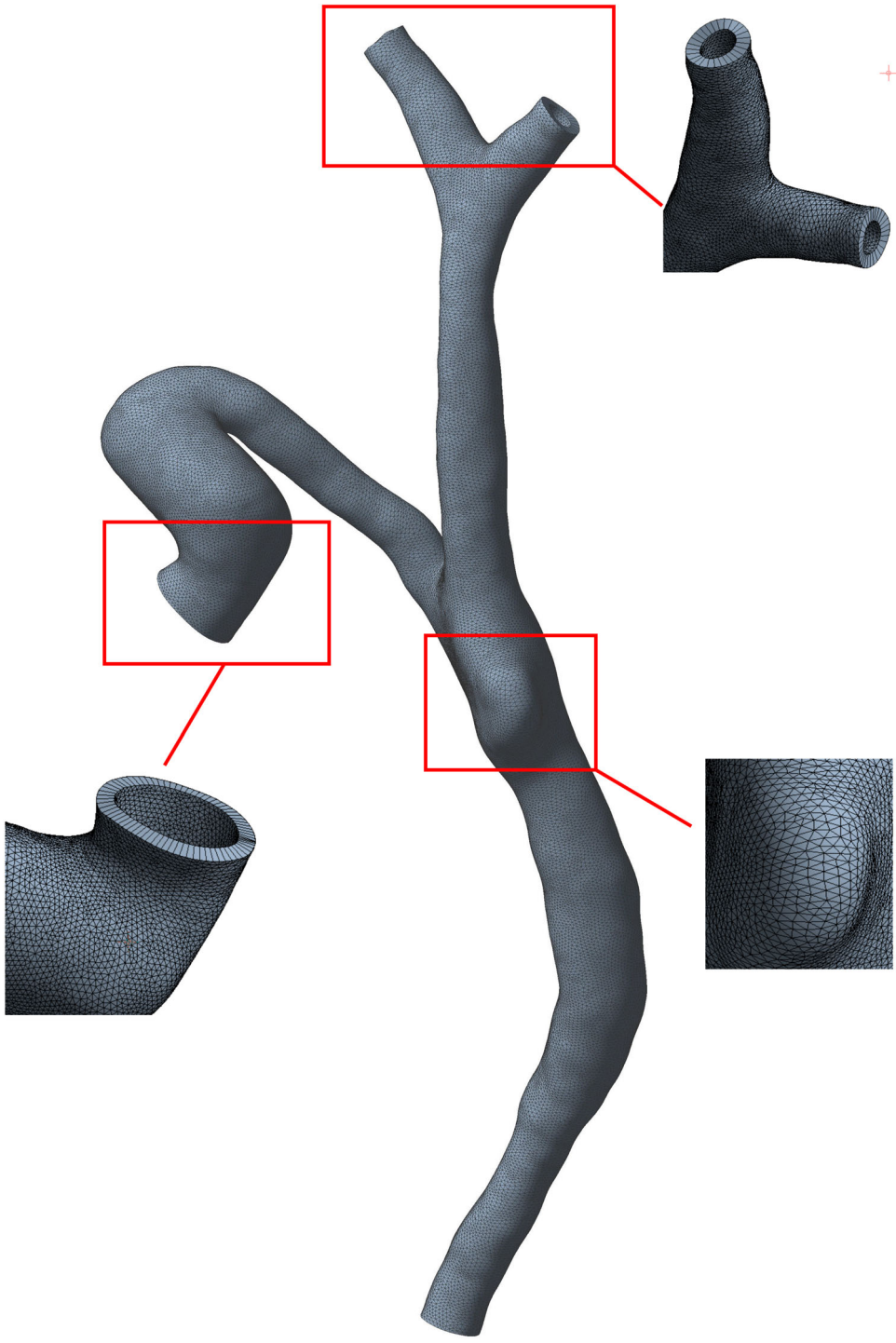

a

Figure 2. Meshes: (a) solid mesh; (b) fluid mesh; (c) comparison between solid and fluid mesh at inlet 2; mesh independency test results in four different densities of meshes: (d) pressure, (e) velocity, (f) wall shear stress.

ratio of each layer 1.3. The inflation layer meshing provides a more accurate resolution of the boundary layer. For certain simulations such as flows with strong wall-bounded effects, this resolution is absolutely necessary. The minimal size of the mesh was 0.3 mm.

The solid mesh was mapped with tetrahedral element sizes of 0.4 mm.

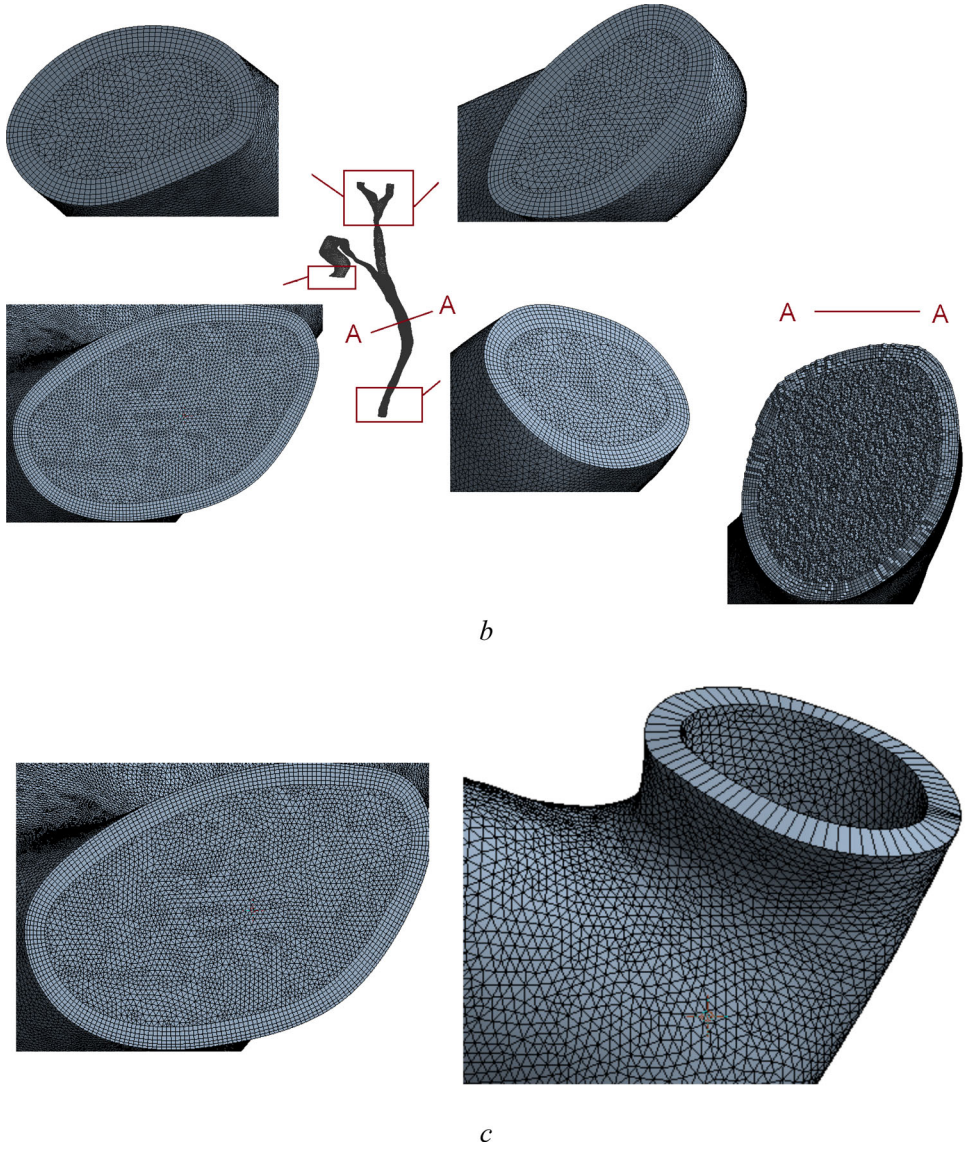

Figure 2. (Continued).

One-way and two-way FSI simulations were performed using ANSYS Workbench 19.0 (ANSYS, Inc., Canonsburg, Pennsylvania, USA).

2.3. Material properties

2.3.1. Mechanical properties of bile duct

The nonlinear response of the bile duct tissue obtained experimentally was detected, and the two-parametric Mooney–Rivlin constitutive model, which is common for soft tissue modelling, was chosen.

$$W = c_{10}\left[\overline{I_1} - 3\right] + c_{01}\left[\overline{I_2} - 3\right] + \frac{1}{d}[J-1]^2, \qquad (1)$$

where W is the strain energy density function, $\overline{I_1}$ and $\overline{I_2}$ are the first and second invariants of the left Cauchy–Green deformation tensor, J is the determinant of the elastic deformation gradient, c_{10} and c_{01} are material parameters and d is the material incompressibility parameter.

Experimental inflation tests of bile ducts have been conducted in Lomonosov Moscow State University. The experimental setup included a polymethylmethacrylate box, two rigid tubes, a pressure sensor, an air compressor and a computer to perform bile duct inflation tests. All experiments were performed at a room temperature of 26 °C. Ethics committee approval was obtained to perform experiments. Sample displacement during inflation was recorded by a camera. Then, the images were processed and parameters of constitutive relation were found. Details of the experiments are described in Appendix 1, supplementary material.

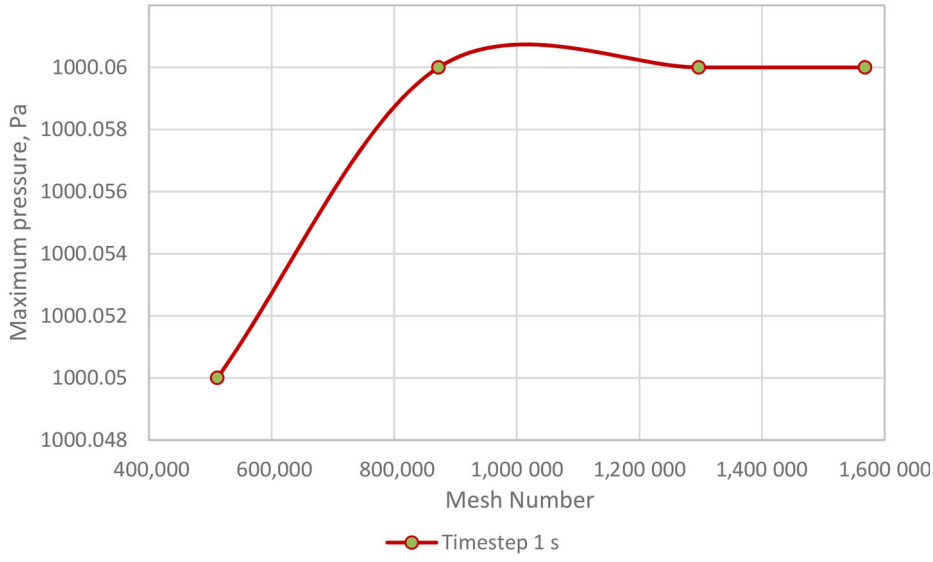

d

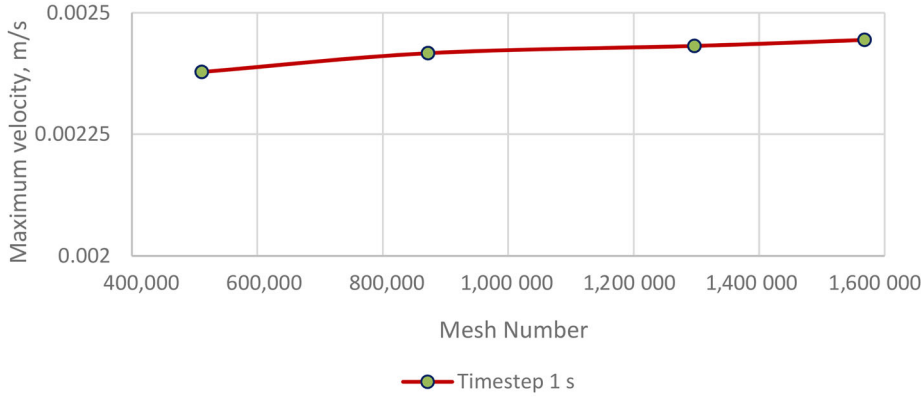

e

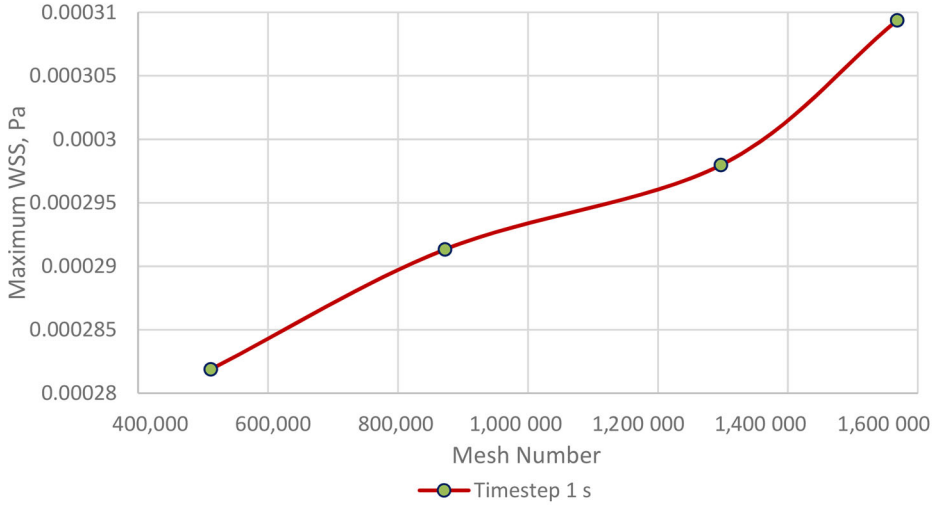

f

Figure 2. (Continued).

Table 2. Constitutive parameters of Mooney-Rivlin model.

c_{10} [kPa]	c_{01} [kPa]	d [Pa^{-1}]
6.34	0.88	0.38

Table 3. Constitutive parameters of the non-Newtonian (Carreau) model for lithogenic bile.

η_0[mPa·s]	η_∞[mPa·s]	a	k
62.5	4.5	0.033	0.56

Table 4. Constitutive parameters of the Newtonian model for healthy bile (Luo et al. 2004; Ooi et al. 2004).

η [mPa·s]	ρ [kg/m^3]
1	1020

Table 2 lists the Mooney–Rivlin constitutive parameters obtained for the present bile duct.

2.3.2. Rheological properties of bile

Lithogenic bile samples were taken from patients at Perm City Clinical Hospital No. 4 as approved by the Hospital Ethics Committee. To determine the rheological characteristics of this biofluid, the Physica MCR 501 (Anton Paar GMbH, Austria) rheometer was adopted. Rheological tests were conducted at 37 °C. The bile was investigated within two to three hours after taking it out from the patients.

The non-Newtonian behaviour of the bile has been implemented by the Carreau model that relates the viscosity, η, as a function of the shear strain rate,$\dot{\gamma}$:

$$\eta = \frac{\eta_0 - \eta_\infty}{\left[1 + (a\dot{\gamma})^2\right]^k} + \eta_\infty \eta \qquad (2)$$

where η_0 is the viscosity at zero shear rate, η_∞ is the viscosity at infinite shear rate, a is the time constant and k is the power index (Table 3). In the case of the healthy bile described as Newtonian fluid, the viscosity was taken equal to 0.001 Pa·s (Table 4) (Luo et al. 2004; Ooi et al. 2004). It was mentioned that normal bile can be regarded as Newtonian fluid (Rodkiewicz et al. 1979; Luo et al. 2004), whereas the lithogenic bile exhibit strong non-Newtonian behaviour (Coene et al. 1994; Kuchumov et al. 2014). Normal bile composition gives a dynamical viscosity and rheology close to water. Pathological state of bile is characterized by the increased content of cholesterol, bile acids, and the mucous substances, which give a major impact to rheology changes. Recent study of lithogenic bile can be found in Minh et al. (2019), where shear-thinning behavior of all samples was revealed. Bile sediment was shown to have has much greater viscosity and stretches more than bile solution. Because mucus concentration makes bile sediment more viscous than the solution, bile viscosity can

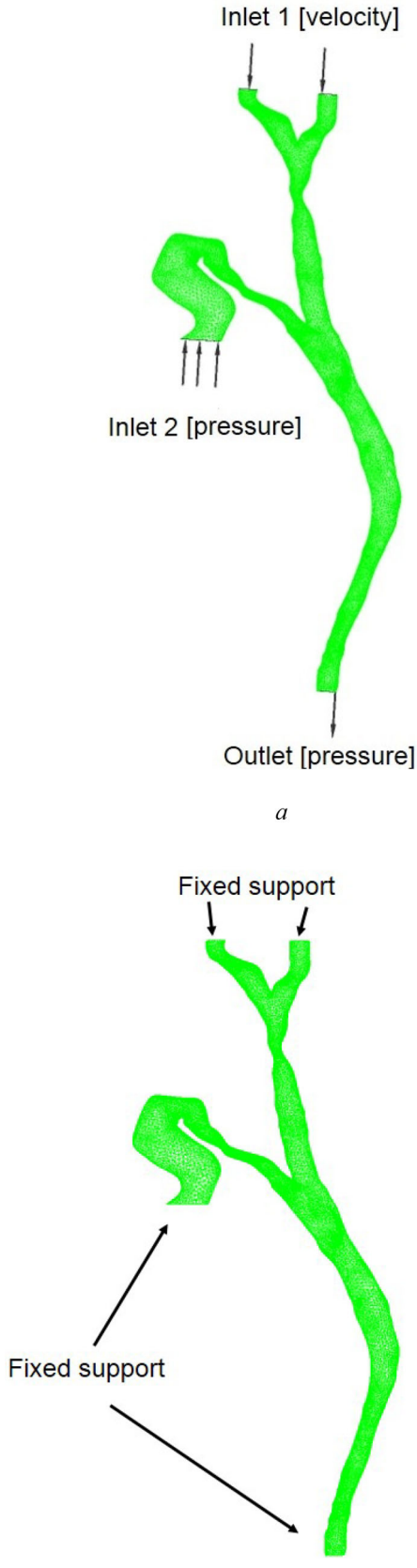

Figure 3. Boundary conditions: (a) fluid mesh; (b) solid mesh.

increase sharply, thereby increasing risks of such diseases as gallstones and sludge build-up in the biliary system.

2.4. Governing equations

The mass and momentum conservation equations for an incompressible fluid can be expressed as

$$\nabla \cdot u = 0, \tag{3}$$

$$\rho_f \left(\frac{\partial u}{\partial t} + \left((u - u_g) \cdot \nabla \right) u \right) = -\nabla p + \nabla \cdot \tau, \tag{4}$$

where ρ_f is the fluid density, p is the pressure, u is the fluid velocity vector and u_g is the moving coordinate velocity. In the arbitrary Lagrangian-Eulerian (ALE) formulation, $(u-u_g)$ is the relative velocity of the fluid with respect to the moving coordinate velocity. Here, τ is the deviatoric shear stress tensor. This tensor is related to the velocity through the strain rate tensor; in the Cartesian coordinates it can be represented as

$$\tau_{ij} = \eta \left(\frac{\partial v_i}{\partial x_j} + \frac{\partial v_j}{\partial x_i} \right), \tag{5}$$

where x_j is the jth spatial coordinate, v_i is the fluid velocity in the direction of axis i, τ_{ij} is the jth component of the stress acting on the faces of the fluid element perpendicular to the axis .

The momentum conservation equation for the solid body can be written as

$$\nabla \cdot \sigma_s = \rho_s \dot{u}_g, \tag{6}$$

where ρ_s, σ_s and $\dot{u}_g$ are density, stress tensor and local acceleration of the solid, respectively.

It is known that blood vessels can be described as hyperelastic materials (Holzapfel et al. 2000; Vassilevski et al. 2015; Amabili et al. 2020). Because of a similar anatomical composition, the bile ducts can also be considered as hyperelastic materials. For hyperelastic materials, the stress–strain relation is written as

$$\sigma_s = \frac{\partial W}{\partial \varepsilon}, \tag{7}$$

where ε is the strain tensor and W is the strain energy density function. The Mooney–Rivlin hyperelastic potential is shown in Equation (1).

The FSI interface should satisfy the following conditions:

1. The displacements of the fluid and solid domain should be compatible, that is, $\delta_s = \delta_f$
2. The tractions at this boundary must be at equilibrium, that is, $\sigma_s \cdot \hat{n}_s = \sigma_f \cdot \hat{n}_f$.
3. The no-slip condition for the fluid should satisfy $u_s = u_f$.

In the above conditions, δ, σ and $\hat{n}$ are displacement, stress tensor and boundary normal, respectively. The subscripts f and s indicate a property of the fluid and solid.

2.5. Boundary conditions

2.5.1. Solid domain

As shown in Figure 3, the edges of the extrahepatic biliary tree were constrained by specifying zero displacements in all directions and prohibiting the rotation about all axes (boundary condition type: fixed support).

2.5.2. Fluid domain

All bile flow cases were examined at the same boundary conditions. Only the gallbladder emptying phase is presented in the paper. Nevertheless, the proposed model enables to simulate the gallbladder refilling phase also. During the gallbladder emptying, the bile flows out from the gallbladder and the liver at the same time. The gallbladder emptying model as modified Windkessel model was proposed by Li et al. (2008b) and adopted here. Also, it can be noted that the gallstones were not modelled directly; instead, the cystic duct lumen decrease was modelled to simulate the stone presence. The laminar flow was noticed. In addition, as the average time to empty a gallbladder with a mean volume of 35 ml of bile is about 30 min according to Dodds et al. (1989) and Al-Atabi et al. (2012) data, this study also assumes that the flow is laminar and that it is sufficiently slow changing to consider that steady state conditions prevail.

The dimensionless Reynolds number is used to determine fluid flow state. Reynolds number (Re) is defined as:

$$Re = \frac{\rho v D}{\mu}, \tag{8}$$

where ρ is the fluid density, v is the velocity of fluid flow, D is the inner diameter of the tube, and μ is the dynamic viscosity.

During computations it was revealed that Reynolds numbers do not exceed value of 40, which corresponds to data of Ooi et al. (2004) and Luo et al. (2007), so the bile flow in the biliary system may be considered as the laminar. The Reynolds number distribution for 1-way and 2-way FSI at time $t = 3$ min is presented in Appendix 4, supplementary material. According to computations, at this time period Reynolds numbers have the maximal value.

Following the work of Howard et al. (Howard et al. 1991), who measured the mean flow rate of the bile from the liver (2.0–3.0 ml/min) after a meal, the flow rate, Q, is calculated accordingly:

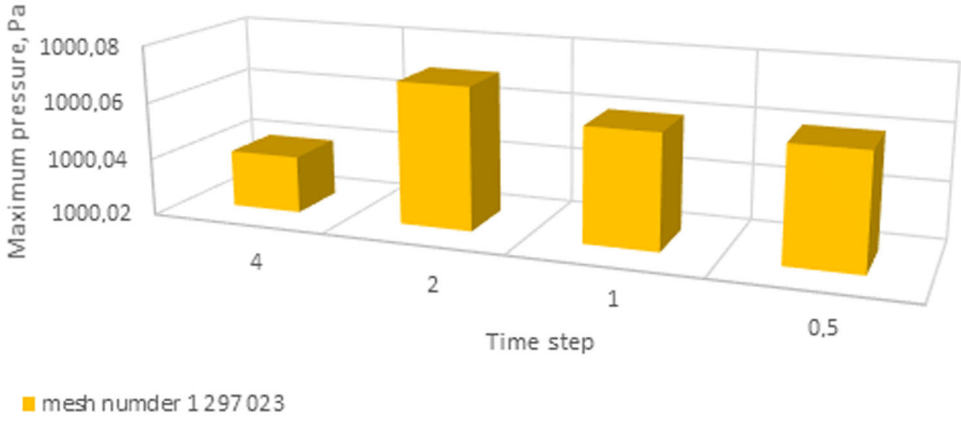

a

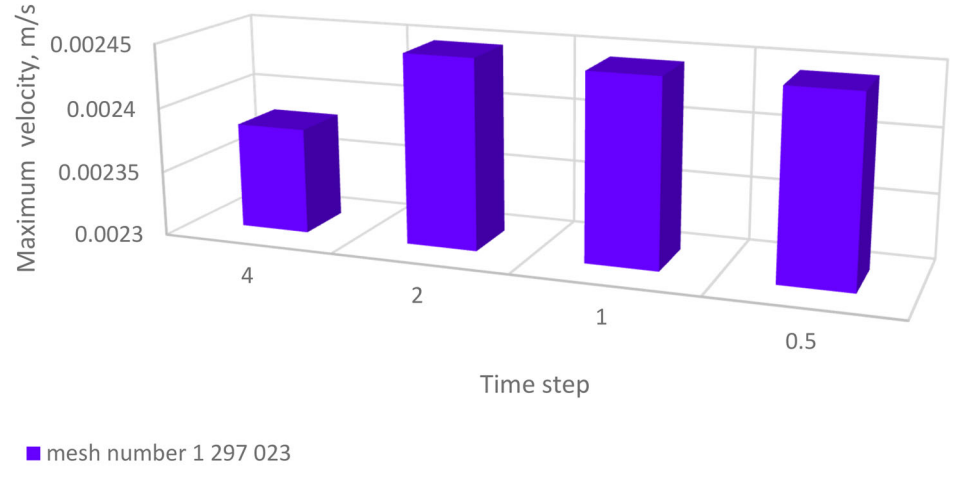

b

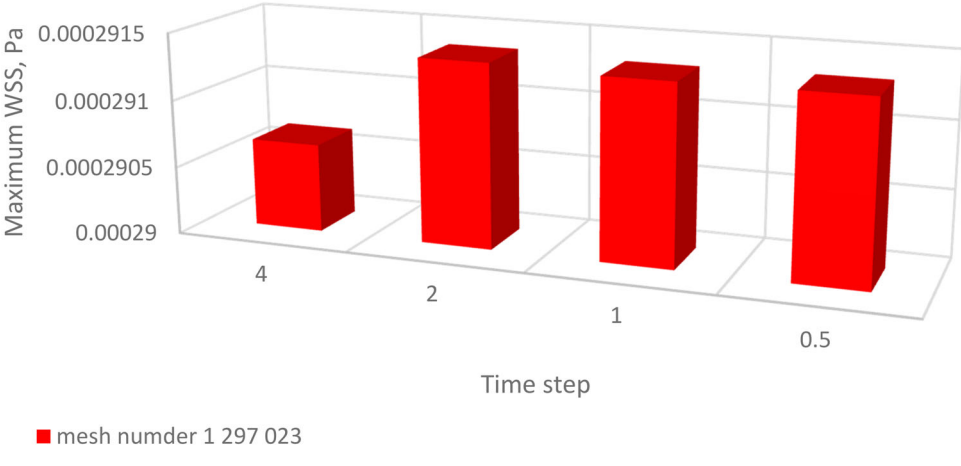

c

Figure 4. Time step dependency test results: (a) pressure, (b) maximal velocity, (c) wall shear stress.

$$Q = \int_S v dS, \tag{9}$$

where v is velocity and S is the cross-sectional area, which can be evaluated for the given patient-specific model. The velocity was obtained from this equation.

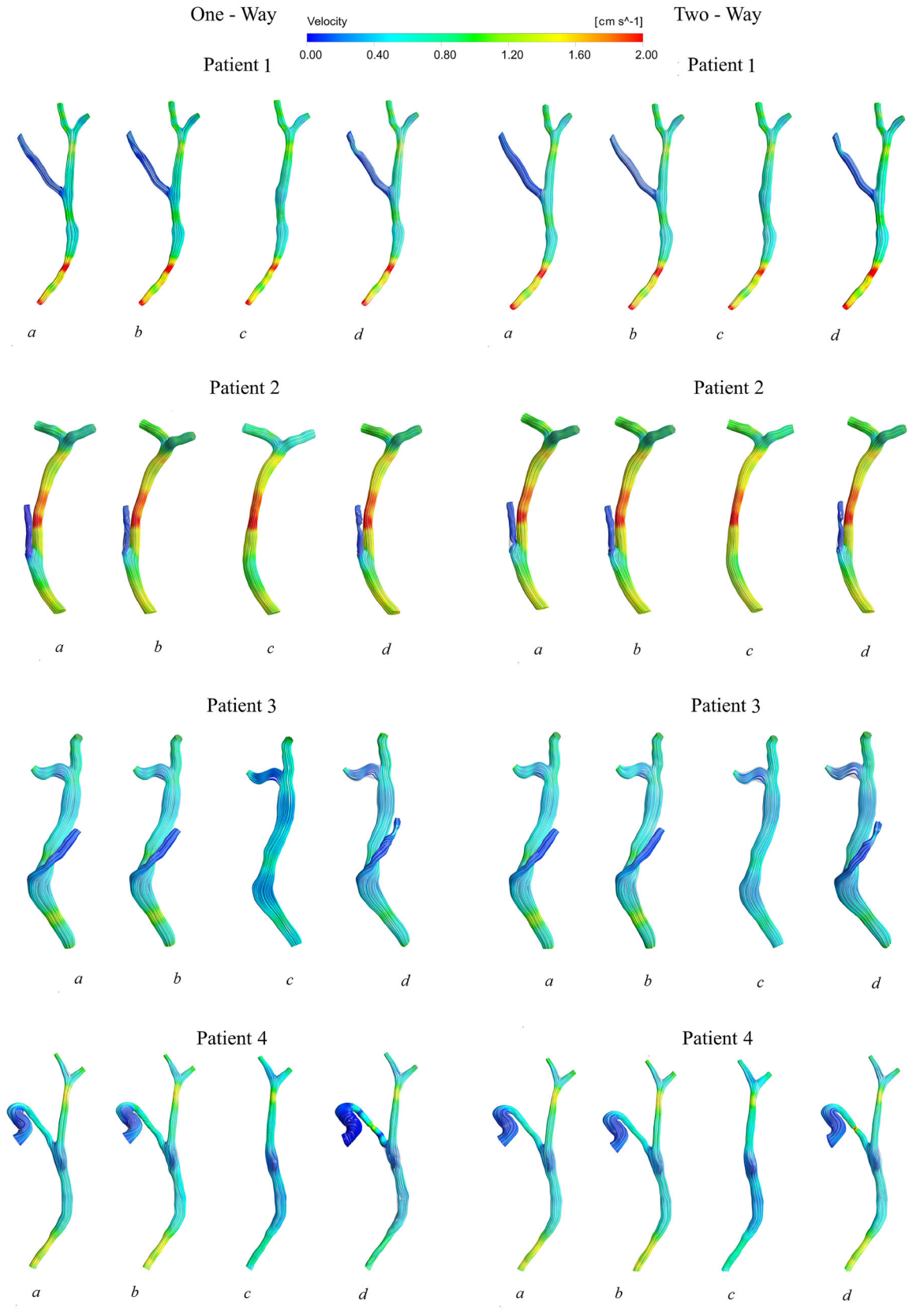

(I)

Figure 5. Velocity distributions along the streamlines at t = 20 min: (I) (a) Newtonian (healthy) bile, (b) lithogenic bile, (c) cholecystectomy, (d) case of the stone presence in the cystic duct; (II) enlarged views of bile flow streamlines in case of d for patient 4 is shown, (III) Comparison between velocities in cases of 1-way and 2-way FSI.

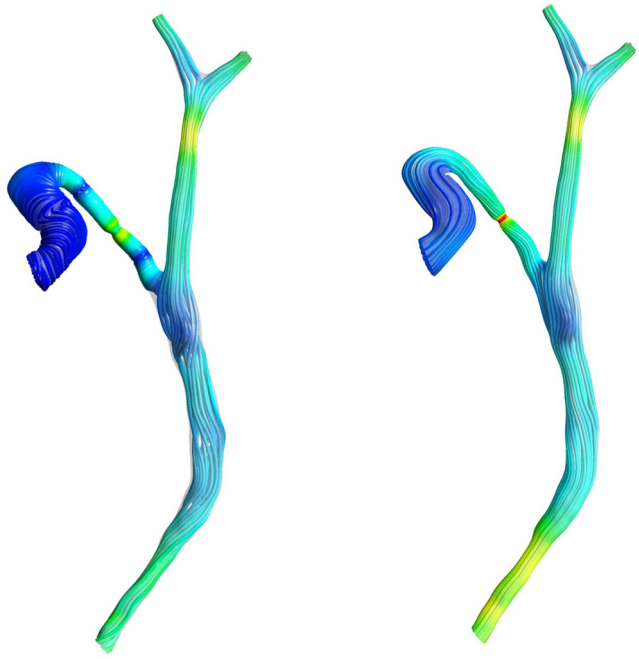

(II)

Figure 5. (Continued).

Subsequently, the mean value of velocity of 3 mm/s was used as inlet 1 velocity. Pressure at the outlet was taken equal to the pressure in the duodenum, that is, 0.96 kPa (Samarcev 2005). The pulsatile flow inlet and pulsatile pressure outlet were not mentioned, because only integrated characteristics for mean flow rate from bile flow out the liver (Howard et al. 1991) and pressure in the duodenum (Samarcev 2005) as an intra-operational measurement were found in the literature. The model assumes to put pulsatile boundary conditions at inlet 1 and outlet in case, if we know patient-specific flow and pressure profiles depending on time.

At inlet 2, the pressure profile corresponding to pressure drop during the gallbladder emptying (Li et al. 2008b) was set:

$$p(t) = p_d + (p_e - p_d)e^{(t_e - t)/RC}, \tag{10}$$

where $p(t)$ is the pressure in the gallbladder, t is time, t_e is the gallbladder emptying time, p_d is the duodenal pressure, p_e is the pressure in the gallbladder with minimal volume (emptying volume), R is the hydraulic resistance, C is the gallbladder wall compliance, $V(t)$ is the gallbladder volume, and V_e is the minimal gallbladder volume (emptying volume). The technique of parameters estimation was described in paper (Kuchumov et al. 2020).

Due to time-dependent boundary conditions and time effects, which can arise during the bile flow in 1-way and 2-way simulations, the transient analysis was adopted.

2.6. Fluid–structure interaction simulation settings

For the FSI, the two solvers, ANSYS Mechanical and ANSYS CFX, were coupled and solved iteratively. In the one-way simulations, the full Newton method with 2400 time iterations using a time step of 1 second was used within the fluid solver to capture the gallbladder emptying time. A sparse matrix solver based on Gaussian elimination was used for solving the system. The fluid field is solved until the convergence criteria were reached. The calculated forces at the structure boundaries were then transferred to the structure side. The structure side was calculated until the convergence criterion was reached: a relative change of 10^{-4} in the norm of all field variables. The solution was finished when the maximum number of time steps was reached.

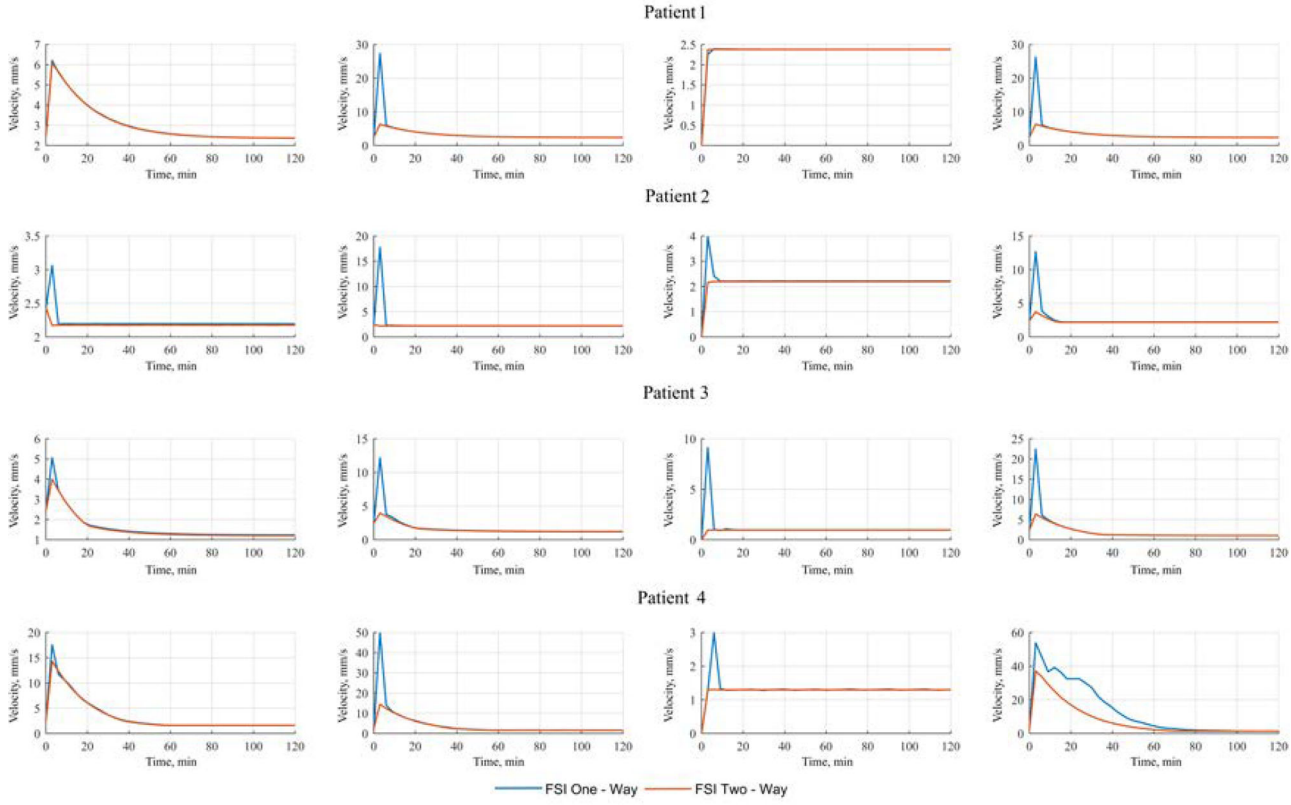

(III)

Figure 5. (Continued).

Two-way FSI algorithm adopted in ANSYS Workbench 19.0 assumed that structural and fluid equations were assembled and solved simultaneously until equilibrium is reached. Physics were coupled by passing loads across fluid-structure interfaces. Transfer from CFD to FEA was using the forces on structure surfaces and backward transfer from FEA to CFD was by displacements of solid structures. The advantage of such approach is that it is necessary to solve each physics in serial or in parallel mode and there is no need to fully converge each intermediate solution. Momentum and mass were chosen as the convergence criteria in case of fluid flow. The convergence criteria were set 10^{-4} for all the variables.

Another parameter that can affect the convergence is the time step size. Changing the time step size for an already-well-converged system needs an appropriate changing in the scale factor in order to reach optimized convergence again. Time step size 1 s was applied to cover total time of simulation, which was taken as 2400s. However, time step sizes 0.5 s, 2 s and 4 s were tested as well in order to get satisfactory rate of convergence. Figure 4 presents the results of time step dependency step analysis for pressure, velocity, and wall shear stress distributions.

Several factors have an influence on the gallbladder emptying rate. An analysis investigated the correlation of maximum % gall bladder volume change between t = 5 and t = 65 min with fat, protein and volume characteristics of the test products and also CCK was performed (Marciani et al. 2013). So, we took 2400s to cover the main processes occurring during the gallbladder emptying. In case of clinical application, the emptying phase simulation time can be changed for each patient based on CCK tests. The model considers it. The middle of simulation time was chosen to visualize the results.

3. Results

3.1. Velocity distributions

Velocity distributions during the gallbladder emptying at t = 20 min is shown in Figure 5. It should be noticed that an increase of maximal bile flow velocities for all patients occurs in a cystic duct with a stenosis due to stone presence. 1-way FSI reveals the swirls in the cystic duct throughout the emptying phase. It is especially pronounced in the patient 4 case. 2-way FSI approach shows more uniform bile

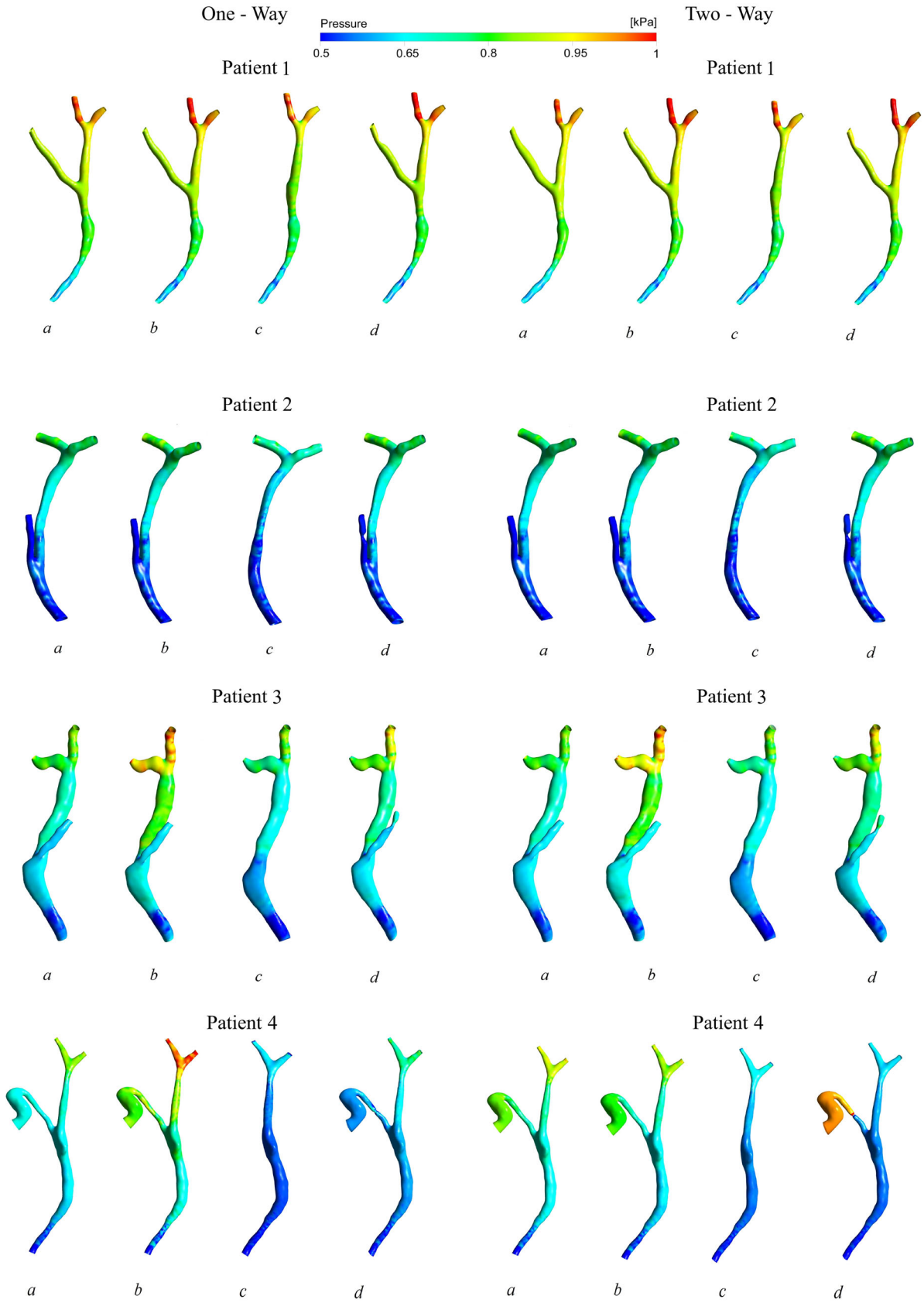

(I)

Figure 6. Pressure distributions at t = 20 min: (I) – (a) Newtonian (healthy) bile, (b) lithogenic bile, (c) cholecystectomy, (d) case of the stone presence in the cystic duct. (II) Comparison between pressure distributions in cases of 1-way and 2-way FSI.

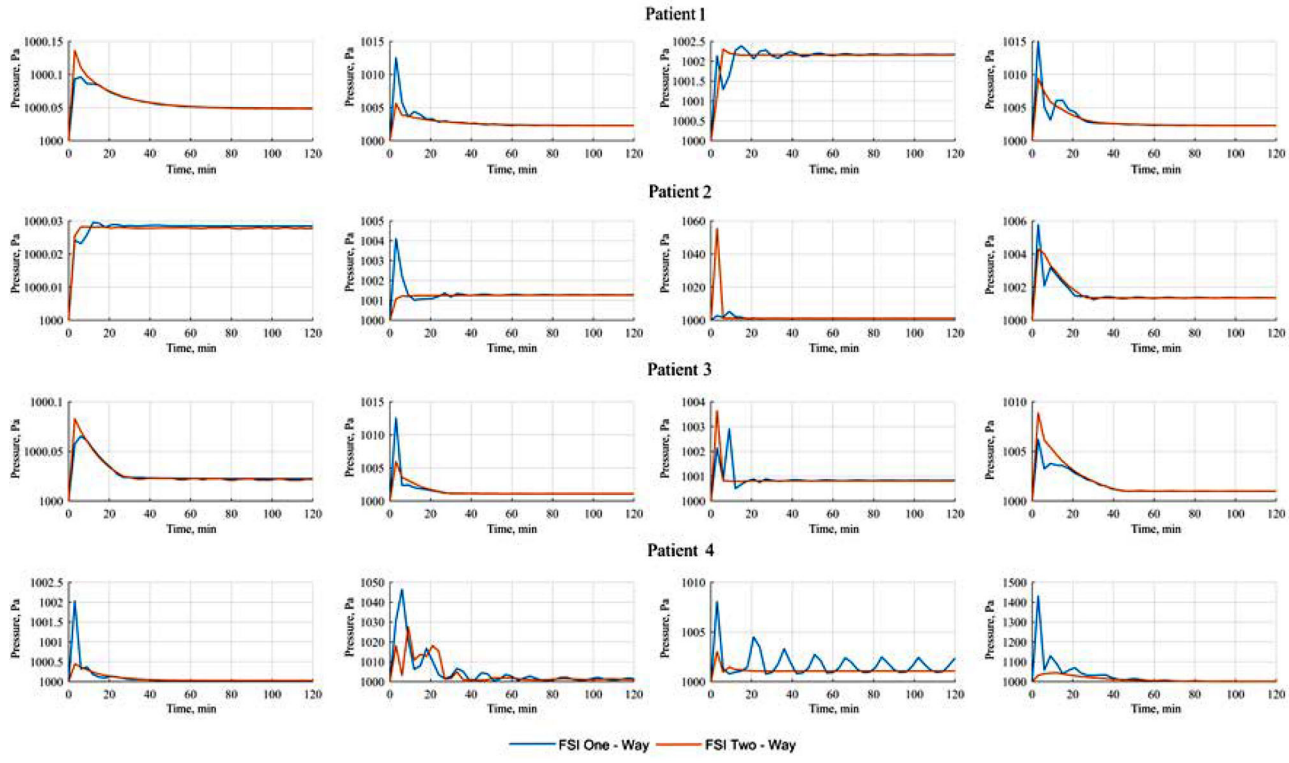

(II)

Figure 6. (Continued).

flow in a cystic duct and close to laminar, which is confirmed by papers (Rodkiewicz and Otto 1979; Al-Atabi et al. 2010). The difference between algorithms is distinctly seen at patient 4 model (Figure 5); enlarged view is also shown in Figure 5.

Figure 5 includes also plots of comparison between velocities as a result of 1-way and 2-way FSI simulations. 2-way FSI provides lower magnitudes compared to 1-way FSI. 1-way FSI demonstrates distinguished peak, which is related with exponent-like boundary condition. Also, one can see the difference between velocity values in cases of different patient-specific geometries. For example, for healthy bile flow case, the maximal velocities are around 6, 3, 5, and 17 mm/s. It can be noticed that in case of stone presence maximal velocities are observed because of acceleration after stenosis region.

3.2. Pressure distributions

The pressure distribution for lithogenic and healthy bile flow is shown in Figure 6. The pressure in the common bile duct in all patients approximately equal to 1 kPa, which corresponds to known medical data (Samarcev 2005; Kuchumov 2016). The changes in bile viscosity and gallbladder presence play a great role in pressure distribution in bile ducts. From a mechanical point of view, the biliary system can be considered to be a pump-pipe system, where the gallbladder provides the driving pressure, and the flow rate of the bile going through the ducts depends on the resistance as well as the pressure drop between the gallbladder and the downstream end of the common bile duct. In this sense, gallbladder motor function is closely related to the pressure drop, flow rate and the flow resistance in the biliary system (Luo et al. 2007).

The motor functions of the gallbladder and biliary tract are closely integrated with the rest of the digestive system by neurohormonal mechanisms that include the vagus and splanchnic nerves and various hormones among them cholecystokinin (CCK). The gallbladder contracting and discharging bile into the duodenum during fasting and digestive periods is controlled by CCK release (Çerçi et al. 2009).

The entry of bile distends the gallbladder by passive and active mechanisms. Adrenergic and

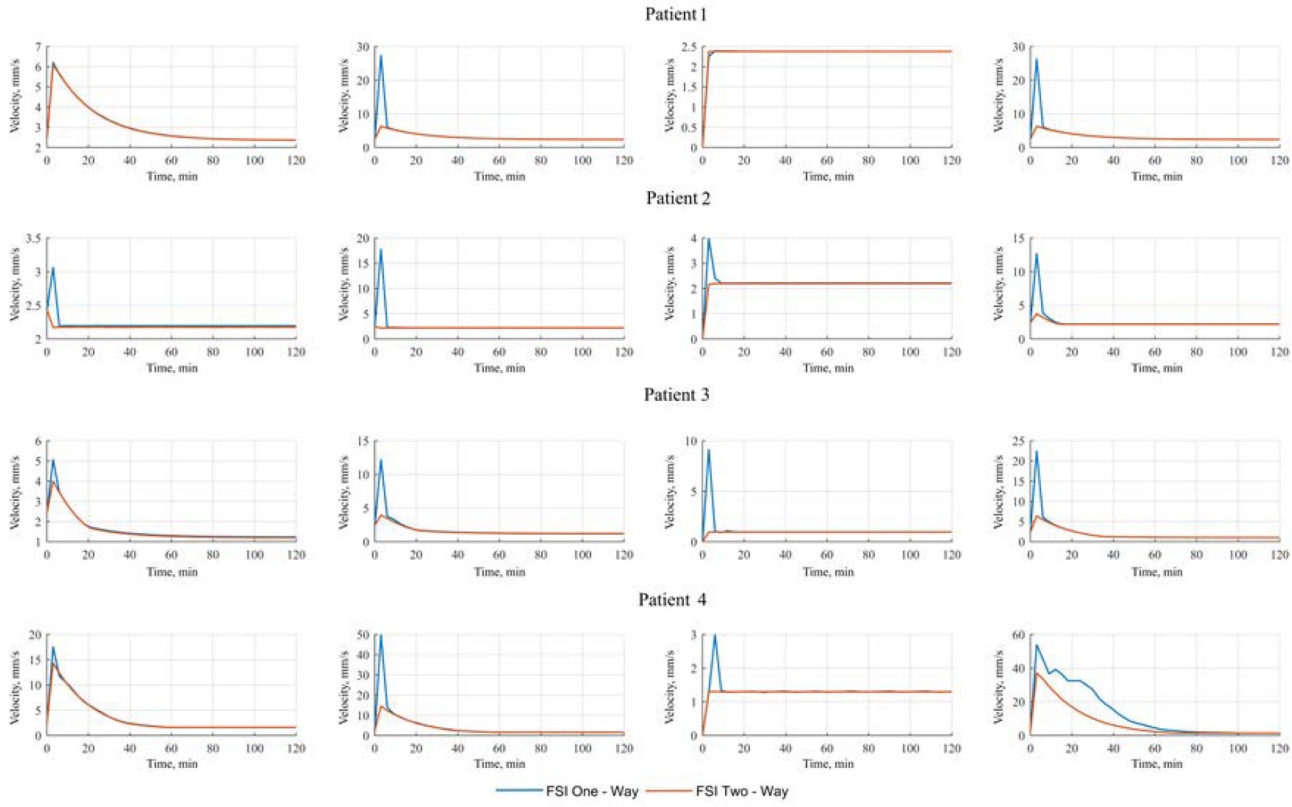

(III)

Figure 6. (Continued).

noncholinergic nonadrenergic nerves mediate the active relaxation or accommodation of the gallbladder that is gradually induced by the incoming bile (Behar 2013). Gallbladder function may be an important predictor of outcome from either cholecystectomy or watchful waiting, because the symptoms traditionally are believed to arise from gallbladder contraction (Larsen and Qvist 2007).

Moreover, it should be noticed that gallbladder absence due to cholecystectomy may lead to different pressure-related complications: sphincter of Oddi disorders (Tanaka et al. 1984), dilatation of the common bile duct (Lv et al. 2015), post-cholecystectomy syndrome (Benias et al. 2018).

The plots of comparison between pressure distribution in cases of 1-way FSI and 2-way FSI is shown in Figure 6.

The lithogenic bile case shows that pressure values are higher in the case of healthy bile flow because of bile viscosity increase in the case of pathology. The stone presence leads to an increase in pressure values in the extrahepatic biliary tree, which is approved by medical evidence in the paper (Csendes et al. 1979).

3.3. Wall shear stress distributions

WSS distributions for bile flow cases are shown in Figure 7. It is known that high velocity regions correspond to increased wall shear stress magnitudes (Oliveira et al. 2019; Yevtushenko et al. 2019). Elevated wall shear stress are observed in the common hepatic duct and common bile duct areas.

Normal physiologic levels of WSS within arteries range from 1 to 7 Pa in vivo, whereas WSS in veins is lower and ranges from 0.1 to 0.6 Pa (Malek et al. 1999). In the case of bile flow, it was shown that WSS changes from 0 to 1.15 Pa. In the case of blood flow, WSS may play a role in the pathogenesis of aneurysmal disease and atherosclerosis development. It is known that lower WSS promotes atherosclerotic plaque development (Samady et al. 2011). In healthy bile flow, the WSS distribution is more intensive compared with the cases where gallstones are present and the bile flow in the extrahepatic biliary tree after cholecystectomy. Influence of bile viscosity on WSS distribution pattern is closely related to the biliary tree geometry. It is also found that the peak value of WSS increases with the increase of bile viscosity, which corresponds with the data obtained for the blood (Wang and Li 2011).

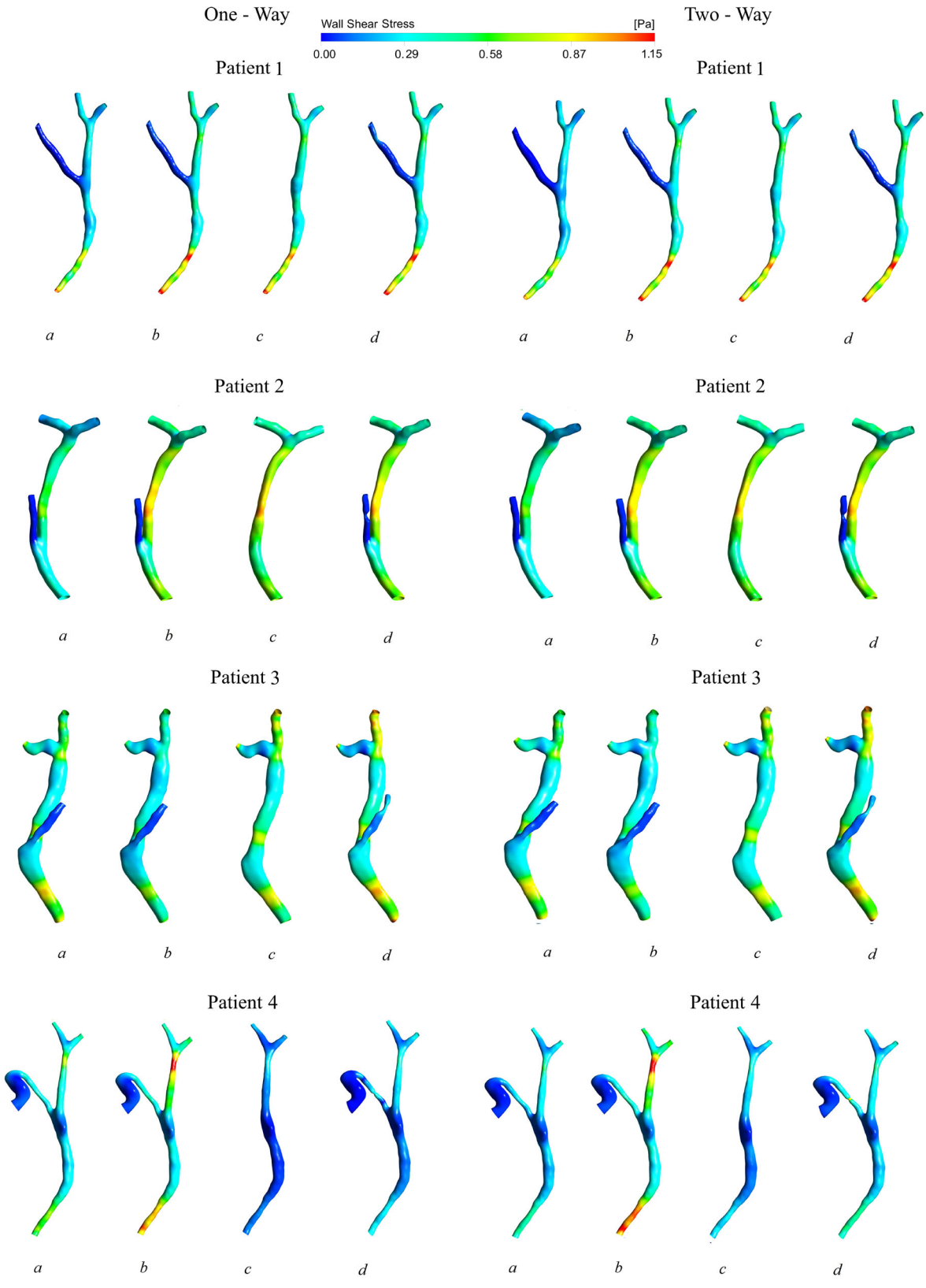

(I)

Figure 7. Wall shear stress distribution at t = 20 min: (a) Newtonian (healthy) bile, (b) lithogenic bile, (c) cholecystectomy, (d) case of the stone presence in the cystic duct.

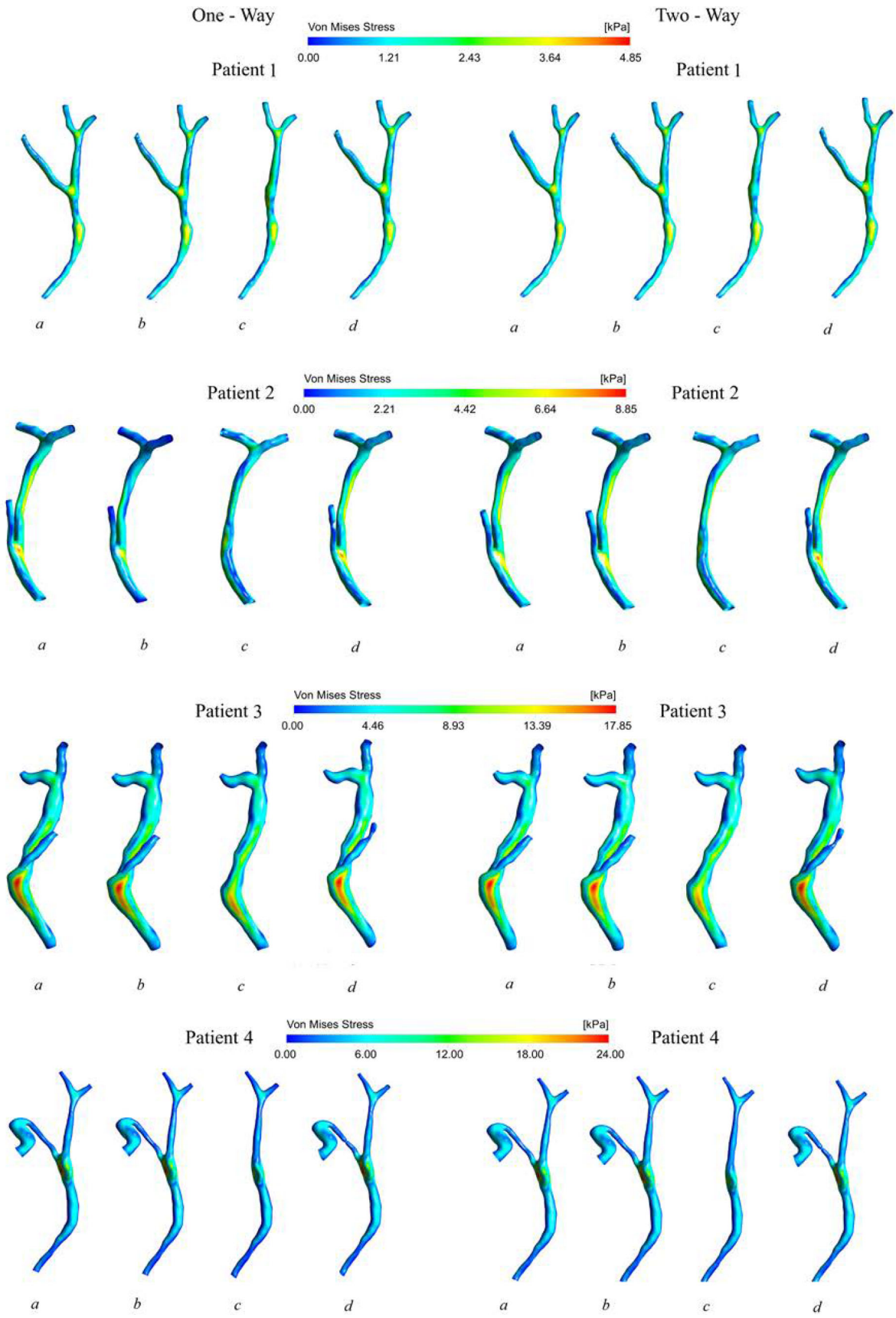

Figure 8. Comparison of results for one-way and two-way couplings, von Mises stress: distribution at t = 20 min: (a) Newtonian (healthy) bile, (b) lithogenic bile, (c) cholecystectomy, (d) case of the stone presence in the cystic duct; also maximal values of von Mises stress in biliary system of patients.

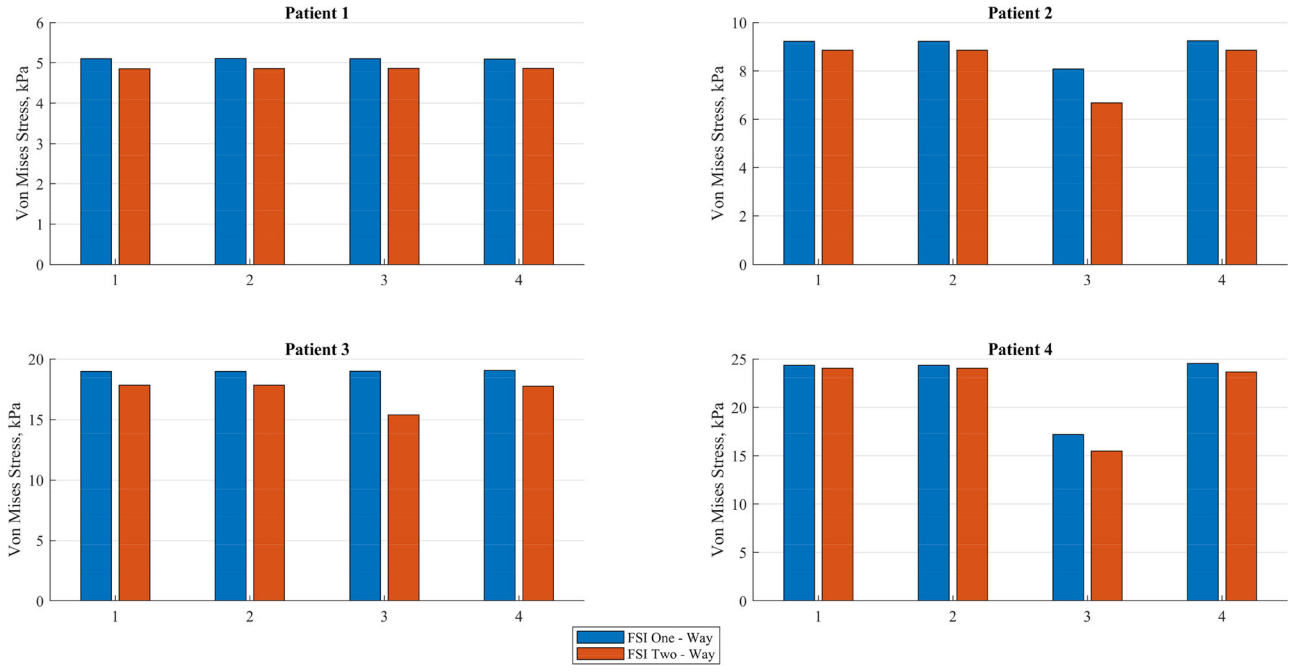

Figure 8. (Continued).

3.4. Von Mises stress distributions

Analysis of distribution characteristics for von Mises Stress is shown in Figure 8. Von Mises Stress distribution slightly differ from the geometry features. Nevertheless, the maximal values of von Mises stress are mostly located in the common bile duct region. It should be noticed that von Mises stress level is much lower compared to blood vessels (Ahmed et al. 2007). Also, it should be noticed that difference of maximal values for various geometries varies from 4.85 to 24 kPa. The cholecystectomy operation does not have an impact on the decreasing of the level of von Mises stress. 1-way and 2-way approaches give approximately the same results here. Nevertheless, 2-way FSI provides the lower magnitudes compared to 1-way FSI. The difference between 1-way and 2-way FSI maximal values of von Mises stress is less than 2%.

4. Discussion

We performed FSI simulation of bile flow in a patient-specific biliary tree, imposing physiological boundary conditions. This model allows us to predict choledynamics of clinical interest in real extrahepatic bile ducts geometry.

In the future, this approach can be used as part of the decision-making support tool in surgery to predict cholecystectomy results.

4.1. Viscosity influence

This is the first study of complex flow in the extrahepatic biliary tree using patient-specific approach. Earlier, only T-tube 1-D approximation was published in Li et al. (2007, 2008a). It was shown there that the 3-D model was more precise than the 1-D model. The comparison between 1-D and 3-D FSI models could be also found in paper (Reymond et al. 2012). The changes of rheological properties led to various flow patterns in the ducts (Kuchumov et al. 2014). The numerical modelling here showed that the difference between bile flow velocities in the healthy state and pathology was not significant. These results were confirmed by paper (Li et al. 2008a), where comparison between Newtonian and non-Newtonian flow in the cystic duct was performed. Nevertheless, there was a difference between pressures in the gallbladder neck area, which was partly confirmed in papers (Body et al. 1996; Samarcev 2005).

4.2. Individual geometry influence

There were no complete data with a complex biliary system to compare with. Nevertheless, there is only one paper devoted to patient-specific modelling in the cystic duct (Al-Atabi et al. 2012). In the present study, we examined 15 patient-specific geometries of various patients in total (4 of which are presented in this paper). The length and thickness of the biliary tree segments were shown to have a serious influence

on flow patterns. It should be noticed that authors in previous papers highlighted the geometry modifications that are very important for bile flow (Bird et al. 2006; Agarwal et al. 2012b). The maximal bile velocity and pressure drop depend mainly on the cystic duct curvature and common bile duct radius. The obtained results for bile flow velocity were compared with the results for a patient-specific bile flow in the cystic duct (Al-Atabi et al. 2012). It can be seen that the flow patterns are the same (the maximal velocity peaks and small vortices can be highlighted). Nevertheless, the values differ. This is because of the different values of boundary conditions applied.

4.3. Wall shear stress

Wall shear stress is one of the most important haemodynamic parameters. There is a great number of papers studying the link between WSS and plaque formation and development (Kwak et al. 2014; Brown et al. 2016; Thondapu et al. 2017). Nevertheless, WSS values for bile duct are still not well studied. The difference between WSS can be explained by the geometrical features of patient-specific models. It should be noticed that WSS values in the bile duct are much lower than of blood vessels (Hoque et al. 2020), namely 1.15 [Pa] versus 7 [Pa] (Malek et al. 1999). It is related with velocities values difference. Maximal WSS can be observed in the common bile duct, which corresponds to the data obtained by Maiti and Misra (2011) and Baghaei et al. (2021). The main challenge is the relationship between WSS and biliary tract pathologies. This paper can be considered as a first step in this direction, but the problem is that we still cannot interpret much of the results. The criteria choice for WSS value in a healthy state and pathology is still a puzzle for the researchers. Recently, a connection between WSS and plastic stent clogging during bile flow was numerically revealed (Kuchumov et al. 2019). In this study, we have shown that elevated values of WSS are observed after cholecystectomy. In the future, WSS in the bile duct can be used as the predictor of gallstone formation and development because of low values, which similar to atherosclerosis formation predictor in the blood vessels (Yevtushenko et al. 2019). Nevertheless, we need more research for numerical value criteria assessment.

4.4. Computational time

The estimated time for conducting 1-way and 2-way coupling numerical simulation of gallbladder emptying was evaluated. It should be noticed that the estimated time of 1-way and 2-way FSI numerical simulation differ by 2 or even 3 times, which corresponds to data published by Benra et al. (2011).

However, it is necessary to notice that the estimated time depends on the technical characteristics of computer technology and the geometric features of the models, which in turn may require a fairly accurate grid model. In this work, HP Pavilion 15-n214sr 8 GB computing technology of 2.1 GHz RAM was used.

4.5. Validation study

Realistic bile flow simulations require corresponding validations against choledynamics. Because there was no available data on bile flow in these geometries, we had to compromise the validation and compare with previous simulation researches known from literature. Despite the difference between the patient-specific geometries, the present simulation results of bile flow model were compared qualitatively with the numerical results of Al-Atabi et al. (2012). Figure 9(a,b) shows the comparison between streamlines in cystic duct during the gallbladder emptying for both studies. It is seen that the present simulation results have the same trend as the earlier results of Al-Atabi et al. (2012). For both studies, the peak of velocity occurs near the cystic duct enter to common hepatic duct. As can be seen, the velocity distributions in the cystic duct are good correlate with each other. It should be noticed that the results have good quantative and qualitive agreement despite difference in the geometry and boundary conditions. It should be emphasized that the present simulations utilized a realistic model of the extra-hepatic biliary tree, while Al-Atabi et al. (2012) used a simplified limited model of the cystic duct that could cause some of the deviation seen.

Moreover, we performed comparison between the variations of pressure difference across the cystic duct for limited model of cystic duct and cystic duct of Al-Atabi et al. (2012) for flow rates of 1, 5, and 10 ml/min. Figure 9(c) shows this comparison. This pressure drop represents the difference between the pressure in the gallbladder and that at the exit of the cystic duct and it is the driving force for emptying the gallbladder. Under physiological conditions, the human bile viscosity, can vary from 1 to roughly 10 mPa s. Therefore, three values (1, 5 and 10 mPa·s) were used to estimate the pressure difference, ΔP across the cystic ducts for various flow rates, Q. The present simulation, however, shows much lower peak pressure

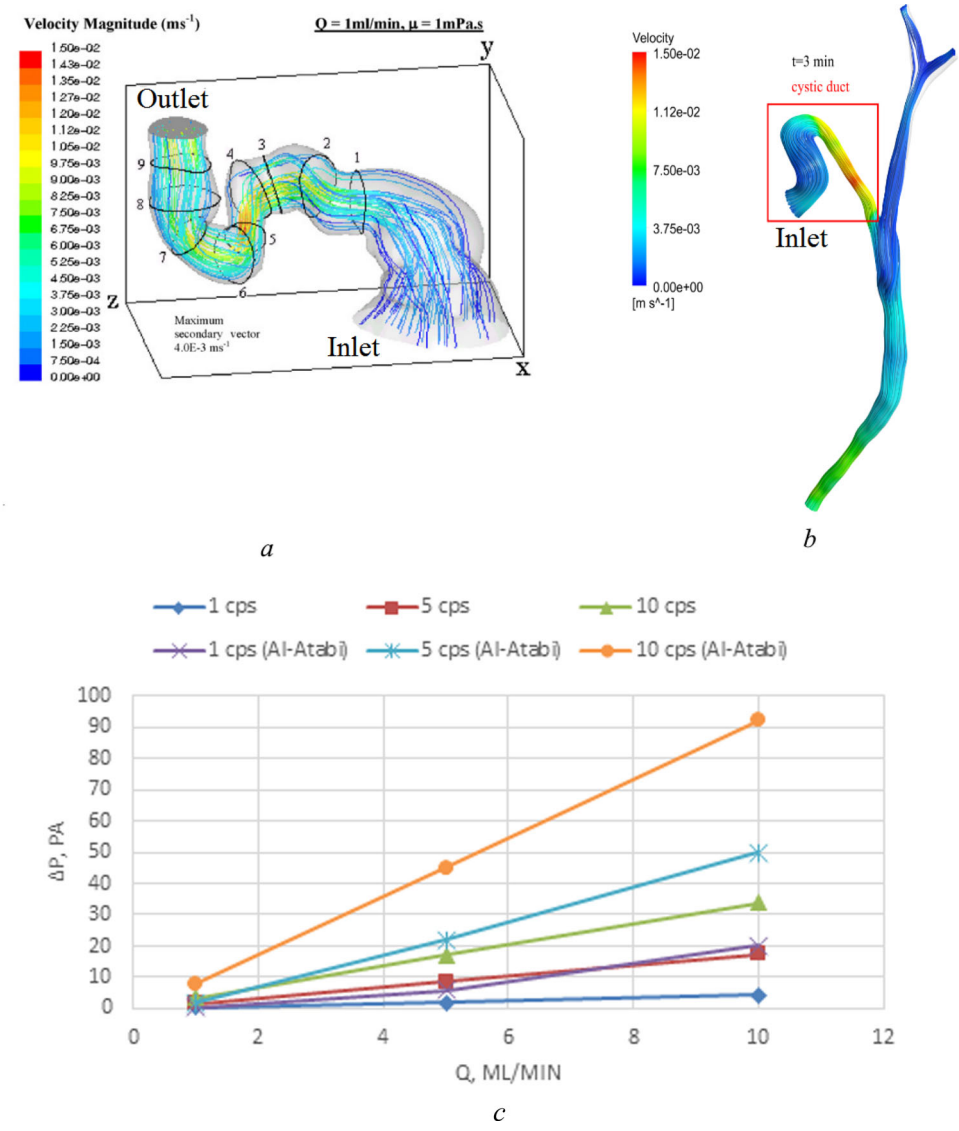

Figure 9. Comparison between streamlines in the cystic duct in the work of (Al-Atabi et al. 2012) (a) and the present study (b). Pressure difference across the cystic duct: comparison of the present FSI solution with the numerical results of (Al-Atabi et al. 2012) (c).

drop. It can be explained by difference in patient-specific geometry. Additionally, It should be noticed that previous research adopted CFD approach, while the present study utilizes 2-way FSI technique.

4.6. Comparison of 1-way and 2-way simulations in biliary system modelling

As it can be seen, the computational time cost at 1-way FSI significantly differs from 2-way FSI computational time in 2 or more times. These differences are related with geometrical features of models and mechanical properties of domains.

Comparing 1-way and 2-way FSI approaches by resulting bile flow pressure and velocities, the difference between algorithms is minimal. The wall shear stress distributions are also identical. Thus, if it is necessary to evaluate the bile flow dynamics in urgent medical situations, 1-way analysis is acceptable.

However, if it is necessary to perform an accurate FEA analysis and evaluate von Mises stress or displacements, etc.) (for example, in case of biliary ducts stenting), it is worth to adopt 2-way FSI (Chandra et al. 2013). Due to complex experimental and clinical in vivo measurements, a precise numerical method for bio-fluid flow description is necessary. The adopted 2-way FSI algorithm is more accurate in comparison with 1-way FSI. It is obvious in the cases with finite deformation and large deflection problems,

where the structural response due to fluid flow effect is clearly seen. Moreover, 1-way FSI approach adoption results in data loss during load and data transfer between analyses (Benra et al. 2011).

In case of bile flow, where the fluid flow does not lead to large deflections, 1-way application can be possible in case of urgent analysis of current medical situation. In case, when the surgeon has a time to evaluate the circumstances of surgical intervention, it is possible to take into account 2-way FSI approach.

Therefore, we can use one-way or two-way FSI techniques based on the considered case depending upon the importance and case sensitivity.

4.7. Clinical applications

The development of non-invasive diagnostic and numerical methods in the contemporary surgery allows to estimate the biomechanical processes in the human body. This circumstance increases the possibility of their use to improve existing and developing new personalized methods for diagnosing and predicting treatment. In particular, there is a growing need for the applications in the biliary system surgery.

It is known that gallbladder surgery leads to 15% of postoperative complications (Radunovic et al. 2016; Taki-Eldin and Badawy 2018). One of the reasons is the use of subjective experience and the lack of individualized biomechanical models for the analysis of surgical interventions.

To predict and prevent postoperative complications, it is necessary to formulate and introduce new technological approaches, which, in particular, may consist in creating a software product (decision-making system in surgical interventions for gallstone disease and its complications). A proposed model of the biliary system makes it possible to assess choledynamics in normal and pathological conditions, as well as to carry out a numerical assessment of bile flow after surgery (removal of the gallbladder) to predict and prevent complications. The results of this study are realized in the decision-making software developed in Perm National Research Polytechnic University. The software enables to evaluate the mean flow rate after cholecystectomy and common bile duct dilatation. These parameters can tell about efficiency of the operation. So, using the results of this paper, the surgeon can evaluate the circumstances of the cholecystectomy for the each patient before operation and evaluate the results of post-operative bile flow features. The details of the developed software and its application in comparison with clinical cases can be found in Appendix 3.

5. Conclusions

The effect of bile pathology on the velocity and pressure distributions in the patient-specific extrahepatic biliary tree was investigated using a one-way FSI and 2-way FSI approaches. Comparisons were made for healthy and lithogenic bile in terms of fluid flow, WSS, pressure, von Mises stress. While no significant differences for velocities between the healthy bile and lithogenic bile cases were present, there was a clear difference when the pressure distribution was compared. Lower values of pressure in the extrahepatic biliary tree in the case of the healthy bile were related to the difference in the rheological properties (the lithogenic bile was more viscous than the healthy bile). WSS distributions were also analysed. It was shown that a more intensive WSS could be seen in the case of healthy bile flow; in pathological cases, lower WSS values were observed. Thus, bile rheology and geometry changes play an important role in the gallbladder disease progression. Moreover, cholecystectomy changes in the bile flow and stress distributions were found. Using a patient-specific model, we numerically showed that velocities and WSS distributions became lower, whereas pressure distributions became higher compared with the healthy state. Therefore, the proposed model could be applied to medical practice to evaluate the circumstances of surgical interventions.

Disclosure statement

No potential conflict of interest was reported by the author(s).

Acknowledgements

Alex G. Kuchumov acknowledges the Perm Region government grant for the development of the scientific school "Computer biomechanics and digital technologies in biomedicine". The work is partly performed in the framework of the development program of the Scientific and Educational Mathematical Center of Privolzhskiy Federal District, project 075-02-2020-1478. The contribution of Vasily Vedeneev into the study of bile duct properties was supported by the Russian Science Foundation (grant No. 19-71-30012). Aleksandr Khairulin acknowledges the financial support of the Ministry of Science and Higher Education of the Russian Federation in the framework of the program of activities of the Perm Scientific and Educational Center "Rational Subsoil Use".

ORCID

Alex G. Kuchumov http://orcid.org/0000-0002-0466-175X
Vasily Vedeneev http://orcid.org/0000-0002-1787-5829
Aleksandr Khairulin http://orcid.org/0000-0002-7506-5568
Oleg Ivanov http://orcid.org/0000-0001-6295-2371

References

Agarwal S, Singh SP. 2016. An analysis of the effect of the peripheral viscosity on bile flow characteristics through cystic duct with stone: study of two-layer model with squeezing. Int J Eng Trends Technol. 32:309–314.

Agarwal S, Sinha AK, Singh SP. 2012a. A theoretical analysis of the effect of the non-Newtonian bile flow on the flow characteristics in the diseased cystic duct. Int J Appl Math Mech. 8:92–103.

Agarwal S, Sinha AK, Singh SP. 2012b. Effect of the plug flow on the flow characteristics of bile through diseased cystic duct: Casson model analysis. Adv Appl Sci Res. 3(2):1098–1106.

Ahamed M, Atique S, Munshi M, Koiranen T. 2017. A concise description of one way and two way coupling methods for fluid-structure interaction problems. Am J Eng Res. 6:86–89.

Ahmed S, Šutalo ID, Kavnoudias H, Madan A. 2007. Fluid structure interaction modelling of a patient specific cerebral aneurysm: effect of hypertension and modulus of elasticity. Proc 16th Australas Fluid Mech Conf 16AFMC. [place unknown]; p. 75–81.

Al-Atabi M, Chin SB, Luo XY. 2010. Experimental investigation of the flow of bile in patient specific cystic duct models. J Biomech Eng. 132:1–6.

Al-Atabi M, Ooi RC, Luo XY, Chin SB, Bird NC. 2012. Computational analysis of the flow of bile in human cystic duct. Med Eng Phys. 34(8):1177–1183. http://dx.doi.org/10.1016/j.medengphy.2011.12.006.

Amabili M, Balasubramanian P, Bozzo I, Breslavsky ID, Ferrari G, Franchini G, Giovanniello F, Pogue C. 2020. Nonlinear dynamics of human aortas for material characterization. Phys Rev X. 10:011015. https://link.aps.org/doi/10.1103/PhysRevX.10.011015.

Baghaei M, Kavian M, Ghodsi S, Razavi SE. 2021. Numerical investigation of bile secretion and pressure rise in obstructed human common bile duct numerical investigation of bile secretion and pressure rise in obstructed human common bile duct. J Appl Fluid Mech. 14:275–286.

Behar J. 2013. Physiology and pathophysiology of the biliary tract: the gallbladder and sphincter of oddi—a review. ISRN Physiol. 2013:1–15. https://www.hindawi.com/journals/isrn/2013/837630/.

Benias PC, Weine DM, Jacobson IM. 2018. Diseases of the bile ducts. In: Lawrence S. Friedman and Paul Martin (Eds.), Handb Liver Dis. Philadelphia: Elsevier; p. 479–498. https://linkinghub.elsevier.com/retrieve/pii/B9780323478748000353.

Benra F-K, Dohmen HJ, Pei J, Schuster S, Wan B. 2011. A comparison of one-way and two-way coupling methods for numerical analysis of fluid-structure interactions. J Appl Math. 2011:1–16. http://www.hindawi.com/journals/jam/2011/853560/.

Bhuvana R, Anburajan M. 2013. Patient specific mimicing CAD models of biliary tract with and without gallstone for CFD analysis of bile dynamics. Int Conf Commun Signal Process ICCSP 2013 - Proc, Melmaruvathur, India. p. 658–662.

Bird NC, Ooi RC, Luo XY, Chin SB, Johnson AG. 2006. Investigation of the functional three-dimensional anatomy of the human cystic duct: a single helix? Clin Anat. 19(6):528–534.

Body L, Højgaard L, Grønvall S, Stage JG. 1996. Human gallbladder pressure and volume: validation of a new direct method for measurements of gallbladder pressure in patients with acute cholecystitis. Clin Physiol. 16(2):145–156.

Brown AJ, Teng Z, Evans PC, Gillard JH, Samady H, Bennett MR. 2016. Role of biomechanical forces in the natural history of coronary atherosclerosis. Nat Rev Cardiol. 13(4):210–220.

Çerçi SS, Özbek FM, Çerçi C, Baykal B, Eroğlu HE, Baykal Z, Yıldız M, Sağlam S, Yeşildağ A. 2009. Gallbladder function and dynamics of bile flow in asymptomatic gallstone disease. WJG. 15(22):2763–2767.

Chandra S, Raut SS, JA, Biederman RW, Doyle M, Muluk SC, Finol EA. 2013. Fluid-structure interaction modeling of abdominal aortic aneurysms: the impact of patient-specific inflow conditions and fluid/solid coupling. J Biomech Eng. 135:81001. https://asmedigitalcollection.asme.org/biomechanical/article/doi/10.1115/1.4024275/371109/FluidStructure-Interaction-Modeling-of-Abdominal.

Coene P-P, Groen AK, Davids PHP, Hardeman M, Tytgat GNJ, Huibregtse K, P-Plo C. 1994. Bile viscosity in patients with biliary drainage. Effect of co-trimoxazole and N-acetylcysteine and role in stent clogging. Scand J Gastroenterol. 29(8):757–763.

Csendes A, Kruse A, Funch-Jensen P, Oster MJ, Ornsholt J, Amdrup E. 1979. Pressure measurements in the biliary and pancreatic duct systems in controls in patients with gallstones, previous cholecystectomy, or common bile duct stones. Gastroenterology. 77(6):1203–1210.

Diehl A. 1991. Epidemiology and natural history of gallstone disease. Gastroenterol Clin North Am. 20(1):1–19.

Dodds WJ, Hogan WJ, Geenen JE. 1989. Motility of the biliary system. In: Schultz S, editor. Handbook of physiology, the gastrointestinal system, motility and circulation. Hoboken, NJ: American Physiological Society; p. 1055–1101.

Ezkurra M, Esnaola JA, Etxeberria U, Lertxundi U, Colomo L, Begiristain M, Zurutuza I. 2018. Analysis of one-way and two-way FSI approaches to characterise the flow regime and the mechanical behaviour during closing manoeuvring operation of a butterfly valve. Int J Mech Mater Eng. 12:409–415.

Holzapfel GA, Gasser TC, Ogden RW. 2000. A new constitutive framework for arterial wall mechanics and a comparative study of material models. J Elast. 61(1/3):1–48.

Hoque KE, Ferdows M, Sawall S, Tzirtzilakis EE. 2020. Engineering the effect of hemodynamic parameters in patient-based coronary artery models with serial stenoses: normal and hypertension cases. Comput Methods Biomech Biomed Eng. 23(9):467–475.

Howard PJ, Murphy GM, Dowling RH. 1991. Gallbladder emptying patterns in response to a normal meal in healthy subjects and patients with gall stones: ultrasound study. Gut. 32(11):1406–1411.

Jahanzamin J, Fatouraee N, Nasiraei-Moghaddam A. 2019. Effect of turbulent models on left ventricle diastolic flow patterns simulation. Comput Methods Biomech Biomed Eng. 22(15):1229–1238.

Kay Washington M. 2009. Gallbladder and extrahepatic bile ducts. In: Noel Weidner, Richard Cote, Saul Suster and Lawrence M. Weiss (Eds.), Modern Surgical Pathology. 2nd edition. Philadelphia: Elsevier Inc.; p. 960–975. http://dx.doi.org/10.1016/B978-1-4160-3966-2.00028-X.

Khan MH, Howard TJ, Fogel EL, Sherman S, Mchenry L, Watkins JL, Canal DF, Lehman GA. 2007. Frequency of biliary complications after laparoscopic cholecystectomy detected by ERCP: experience at a large tertiary referral center. Gastrointest Endosc. 65(2):247–252.

Kuchumov AG. 2016. Mathematical modeling of the peristaltic lithogenic bile flow through the duct at papillary stenosis as a tapered finite-length tube. Russ J Biomech. 20:77–96.

Kuchumov AG. 2019. Biomechanical model of bile flow in the biliary system. Russ J Biomech. 23:224–248.

Kuchumov AG, Gilev V, Popov V, Samartsev V, Gavrilov V. 2014. Non-Newtonian flow of pathological bile in the biliary system: experimental investigation and CFD simulations. Korea-Aust Rheol J. 26(1):81–90.

Kuchumov AG, Kamaltdinov M, Selyaninov A, Samartsev V. 2019. Numerical simulation of biliary stent clogging. Ser Biomech. 33:3–15.

Kuchumov AG, Kamaltdinov MR, Samartsev VA, Khairulin AR, Ivashova YA, Taiar R. 2020. Patient-specific simulation of a gallbladder refilling based on MRI and ultrasound in vivo measurements. AIP Conf Proc 2216: 060004. http://aip.scitation.org/doi/abs/10.1063/5.0003367.

Kuchumov AG, Nyashin YI, Samarcev VA, Gavrilov VA. 2013a. Modelling of the pathological bile flow in the duct with a calculus. Acta Bioeng Biomech. 15:9–17.

Kuchumov AG, Nyashin YI, Samartsev VA. 2013b. CFD approach to bile flow problems solution. 18th Int Symp Comput Biomech Ulm; May 13–14; Ulm. p. 67–68.

Kuchumov AG, Nyashin YI, Samartsev VA. 2015. Modelling of peristaltic bile flow in the papilla ampoule with stone and in the papillary stenosis case: application to reflux investigation. In: Goh J, Lim CT, editors. Proc 7th WACBE World Congress on Bioengineering Singapore, 2015. p. 158–161. Switzerland: Springer International Publishing.

Kuchumov AG, Nyashin YI, Samartsev VA, Gavrilov VA. Mesnard M. 2011. Biomechanical approach to biliary system modelling as a step towards "Virtual Physiological Human" project. Russ J Biomech. 15:28–42. http://vestnik.pstu.ru/biomech/archives/?id=&folder_id=2160.

Kwak BR, Bäck M, Bochaton-Piallat M-L, Caligiuri G, Daemen MJAP, Davies PF, Hoefer IE, Holvoet P, Jo H, Krams R, et al. 2014. Biomechanical factors in atherosclerosis: mechanisms and clinical implications. Eur Heart J. 35(43):3013–3020.

Larsen TK, Qvist N. 2007. The influence of gallbladder function on the symptomatology in gallstone patients, and the outcome after cholecystectomy or expectancy. Dig Dis Sci. 52(3):760–763.

Li WG, Luo XY, Chin SB, Hill NA, Johnson AG, Bird NC. 2008a. Non-Newtonian bile flow in elastic cystic duct: one- and three-dimensional modeling. Ann Biomed Eng. 36(11):1893–1908.

Li WG, Luo XY, Hill NA, Smythe A, Chin SB, Johnson a. G, Bird N. 2008b. Correlation of mechanical factors and gallbladder pain. Comput Math Methods Med. 9(1): 27–45. http://www.hindawi.com/journals/cmmm/2008/270169/.

Li WG, Luo XY, Johnson AG, Hill NA, Bird N, Chin SB. 2007. One-dimensional models of the human biliary system. J Biomech Eng. 129(2):164–173.

Lo RC, Huang WL, Fan YM. 2015. Evaluation of bile reflux in HIDA images based on fluid mechanics. Comput Biol Med. 60:51–65.

Luo X, Li W, Bird N, Chin SB, Hill NA, Johnson AG. 2007. On the mechanical behavior of the human biliary system. WJG. 13(9):1384–1392.

Luo XY, Chin SB, Ooi RC, Clubb M, Johnson AG, Bird N. 2004. The rheological properties of human bile. In: Recent Advances in Fluid Mechanics: Proceedings of the Fourth International Conference on Fluid Mechanics 20-23 July, 2004, Dalian, China. Beijing: Tsinghua University Press; p. 876.

Lv Y, Lau W, Wu H, Chang S, NingLiu N, Li Y, Deng J. 2015. Etiological causes of intrahepatic and extrahepatic bile duct dilatation. Int J New Technol Res. 1:263634.

Maiti S, Misra JC. 2011. Peristaltic flow of a fluid in a porous channel: a study having relevance to flow of bile within ducts in a pathological state. Int J Eng Sci. 49(9): 950–966. http://dx.doi.org/10.1016/j.ijengsci.2011.05.006.

Malek AM, Alper SL, Izumo S. 1999. Hemodynamic shear stress and its role in atherosclerosis. JAMA. 282(21): 2035–2042.

Marakhovskiy Y. 2003. Gallbladder disease: current state. Russ J Gastroentorology Hepatol Coloproctol. 13:81–92. In Russian.

Marciani L, Cox EF, Hoad CL, Totman JJ, Costigan C, Singh G, Shepherd V, Chalkley L, Robinson M, Ison R, et al. 2013. Effects of various food ingredients on gall bladder emptying. Eur J Clin Nutr. 67:1182–1187. http://dx.doi.org/10.1038/ejcn.2013.168.

Minh NN, Obara H, Shimokasa K, Zhu J. 2019. Tensile behavior and extensional viscosity of bile. Biorheology. 56(4):237–252. https://www.medra.org/servlet/aliasResolver?alias=iospress&doi=10.3233/BIR-190216.

Mohan S, Shashidhara T, Sahil M, Akarsh R. 2014. Gallbladder stones: surgical treatment. Int J Res Med Sci. 2(1):285. http://www.scopemed.org/?mno=48209.

Oliveira D, Rosa SA, Tiago J, Ferreira RC, Agapito AF, Sequeira A. 2019. Bicuspid aortic valve aortopathies: an hemodynamics characterization in dilated aortas. Comput Methods Biomech Biomed Eng. 22(8):815–826.

Ooi RC, Luo XY, Chin SB, Johnson AG, Bird NC. 2004. The flow of bile in the human cystic duct. J Biomech. 37(12):1913–1922. http://dx.doi.org/10.1016/j.jbiomech.2004.02.029.

Opie EL. 1901. The relation of cholelithiasis to disease of the pancreas and to fat necrosis. Johns Hopkins Hosp Bull. 12:19–21.

Portincasa P, Moschetta A, Palasciano G. 2006. Cholesterol gallstone disease. Lancet. 368(9531):230–239.

Qiao Y, Zeng Y, Ding Y, Fan J, Luo K, Zhu T. 2019. Numerical simulation of two-phase non-Newtonian blood flow with fluid-structure interaction in aortic dissection. Comput Methods Biomech Biomed Eng. 22(6): 620–630.

Radunovic M, Lazovic R, Popovic N, Magdelinic M, Bulajic M, Radunovic L, Vukovic M, Radunovic M. 2016. Complications of laparoscopic cholecystectomy: our experience from a retrospective analysis. Open Access Maced J Med Sci. 4(4):641–646.

Reymond P, Crosetto P, Deparis S, Quarteroni A, Stergiopulos N. 2012. Physiological simulation of blood flow in the aorta: comparison of hemodynamic indices as predicted by 3-D FSI, 3-D rigid wall and 1-D models. Med Eng Phys. 35:1–8.

Rodkiewicz CM, Otto WJ. 1979. On the Newtonian behavior of bile. J Biomech. 12(8):609–612.

Rodkiewicz CM, Otto WJ, Scott GW. 1979. Empirical relationships of bile. J Biomech. 12(6):411–413.

Samady H, Eshtehardi P, McDaniel MC, Suo J, Dhawan SS, Maynard C, Timmins LH, Quyyumi AA, Giddens DP. 2011. Coronary artery wall shear stress is associated with progression and transformation of atherosclerotic plaque and arterial remodeling in patients with coronary artery disease. Circulation. 124(7):779–788.

Samarcev VA. 2005. Paths of the improvement of the cholelithiasis treatment at the high operative risk groups: optimization of the diagnostics methods, landmark endoscopic and less-invasive tratment, predicting and prophylactics of the complications. Perm, Russian Federation: Academician EA Wagner Perm State Medical Academy.

Stinton LM, Shaffer EA. 2012. Epidemiology of gallbladder disease: cholelithiasis and cancer. Gut Liver. 6(2): 172–187.

Taki-Eldin A, Badawy AE. 2018. Outcome of laparoscopic cholecystectomy in patients with gallstone disease at a secondary level care hospital. Arq Bras Cir Dig. 31:e1347.

Tanaka M, Ikeda S, Nakayama F. 1984. Change in bile duct pressure responses after cholecystectomy: loss of gallbladder as a pressure reservoir. Gastroenterology. 87(5):1154–1159. http://dx.doi.org/10.1016/S0016-5085. (84)80078-5

Tao X, Gao P, Jing L, Lin Y, Sui B. 2015. Subject-specific fully-coupled and one-way fluid-structure interaction models for modeling of carotid atherosclerotic plaques in humans. Med Sci Monit. 21:3279–3290. http://www.medscimonit.com/abstract/index/idArt/895137.

Thondapu V, Bourantas CV, Foin N, Jang IK, Serruys PW, Barlis P. 2017. Basic science for the clinician: biomechanical stress in coronary atherosclerosis: emerging insights from computational modelling. Eur Heart J. 38:81–92.

Vassilevski YV, Salamatova VY, Simakov SS. 2015. On the elasticity of blood vessels in one-dimensional problems of hemodynamics. Comput Math Math Phys. 55(9):1567–1578. Available from: http://link.springer.com/10.1134/S0965542515090134.

Wang X, Li X. 2011. Computational simulation of aortic aneurysm using FSI method: influence of blood viscosity on aneurismal dynamic behaviors. Comput Biol Med. 41(9):812–821. http://dx.doi.org/10.1016/j.compbiomed.2011.06.017.

Xu K, Yu L, Wan J, Wang S, Lu H. 2020. The influence of the elastic modulus of the plaque in carotid artery on the computed results of FFRCT. Comput Methods Biomech Biomed Eng. 23(5):201–211.

Yevtushenko P, Hellmeier F, Bruening J, Nordmeyer S, Falk V, Knosalla C, Kelm M, Kuehne T, Goubergrits L. 2019. Surgical aortic valve replacement: are we able to improve hemodynamic outcome? Biophys J. 117(12):2324–2336.